Manuscript Details

Manuscript number	FORC_2018_66_R1
Title	Paper characteristics and their influence on the ability of Single Metal Deposition to detect fingermarks
Short title	Paper and detection of fingermarks
Article type	Full Length Article

Abstract

This study aims at exploring the way paper samples may impact the performance of Single-Metal Deposition (SMD II), a fingermark detection technique known for its versatility of application as well as its sensitivity regarding porous substrates. To get a broader view on how porous substrates may impact the SMD II performances, 74 North American and European papers types were collected, characterized (UV-visible and infrared spectroscopy, roughness, porosity, and surface pH), and processed as substrates bearing fingermarks. This part of the study represented a first valuable outcome by the number of samples considered. After processing with SMD II, the samples were characterized again with the techniques mentioned above, background staining and fingermark quality were assessed and associated with a quality score. Overall, no positive nor negative trend was observed between the paper characteristics and the SMD II performance. As a consequence, it is currently still not possible to predict if a paper sample will behave well or bad with SMD II. Of all the monitored parameters, the chemical composition of the surface coating (i.e., silica or calcium carbonate) may be worth exploring further, as it has been observed that some coatings undergo partial degradation during the SMD II process. As a result, secretion residue may be damaged by the chemical solubilization of the support layer if they failed to penetrate deeper into the substrate.

Keywords	TRL level 3 Forensic Science; Chemical analysis; Porous substrate; Surface properties; Gold Nanoparticles
Manuscript category	Technology Readiness Level 3

Corresponding Author	Sylvain Robert
Corresponding Author's Institution	UQTR
Order of Authors	Ouahiba Acherar, Minh Quang Truong, Sylvain Robert, Frank CRISPINO, Sebastien Moret, Andy Bécue
Suggested reviewers	Alexandre Beaudoin, Della Wilkinson, Stephen Bleay

Submission Files Included in this PDF

File Name [File Type]

Manuscript_final_Highlights.docx [Highlights]

Manuscript Graphical Abstract.tif [Graphical Abstract]

Manuscript_final.docx [Manuscript File]

Manuscript_final_Figures.docx [Figure]

FORC-AUTHOR-DECLARATION.docx [Conflict of Interest]

Manuscript_final_Appendices.docx [Supporting File]

To view all the submission files, including those not included in the PDF, click on the manuscript title on your EVISE Homepage, then click 'Download zip file'.

Research Data Related to this Submission

There are no linked research data sets for this submission. The following reason is given:
The authors are unable or have chosen not to specify which data has been used

Highlights

- Physical surface topography (roughness and porosity) as well as cellulose and lignin chemical groups have no detectable influence on fingermarks detection using the SMDII technique
- The only factor that may be of importance seems to be the chemical composition of surface coating (silicates and carbonates).

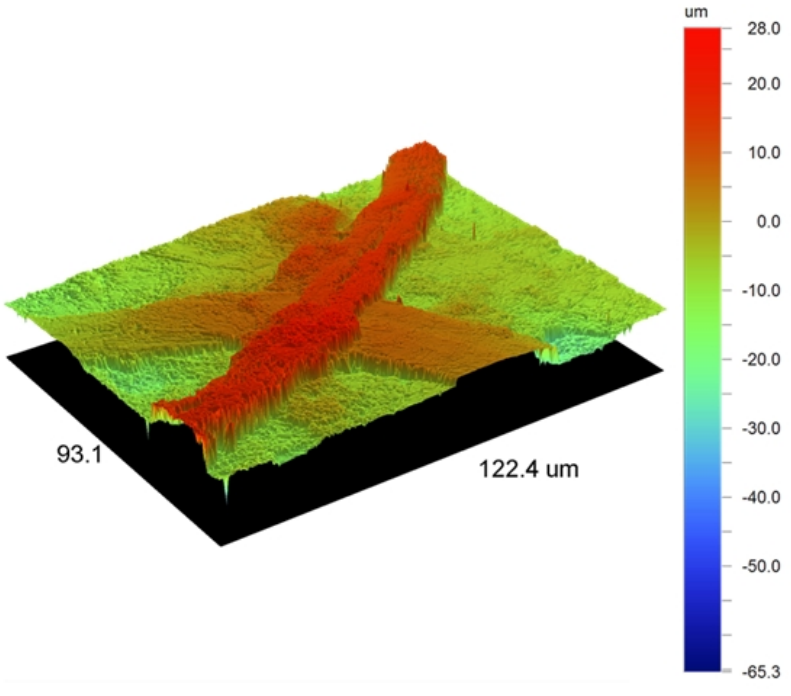
um
28.0
20.0
10.0
0.0
-10.0
-20.0
-30.0
-40.0
-50.0
-65.3
93.1
122.4 um

Article type: Full length article

TRL level: 3

Title

Paper characteristics and their influence on the ability of Single Metal Deposition to detect fingermarks

Authors

Ouahiba ACHERAR [a]

Minh Quang TRUONG [b]

Sylvain ROBERT [a] *

Frank CRISPINO [a, d]

Sébastien MORET [b, c (present address)]

Andy BÉCUE [b]

(*) corresponding author

Affiliations

[a] Laboratoire de recherche en criminalistique; Département de chimie, biochimie et physique; Université du Québec à Trois-Rivières, QC, Canada, G9A 5H7

[b] École des sciences criminelles; Faculté de droit, des sciences criminelles et d'administration publique; Bâtiment Batochime, Université de Lausanne, CH-1015 Lausanne-Dorigny, Switzerland

[c] University of Technology Sydney, Centre for Forensic Science, Broadway 2007, Australia

[d] Centre international de criminologie comparée, Université du Québec à Trois-Rivières, QC, Canada, G9A 5H7

Email addresses

Sylvain ROBERT (Sylvain.Robert@videotron.ca, Sylvain.Robert@uqtr.ca)

Frank CRISPINO (Frank.Crispino@uqtr.ca)

Sébastien MORET (Sebastien.Moret@uts.edu.au)

Andy BÉCUE (Andy.Becue@unil.ch)

Abstract

This study aims at exploring the way paper samples may impact the performance of Single-Metal Deposition (SMD II), a fingermark detection technique known for its versatility of application as well as its sensitivity regarding porous substrates. To get a broader view on how porous substrates may impact the SMD II performances, 74 North American and European papers types were collected, characterized (UV-visible and infrared spectroscopy, roughness, porosity, and surface pH), and processed as substrates bearing fingermarks. This part of the study represented a first valuable outcome by the number of samples considered. After processing with SMD II, the samples were characterized again with the techniques mentioned above, background staining and fingermark quality were assessed and associated with a quality score. Overall, no positive nor negative trend was observed between the paper characteristics and the SMD II performance. As a consequence, it is currently still not possible to predict if a paper sample will behave well or bad with SMD II. Of all the monitored parameters, the chemical composition of the surface coating (*i.e.*, silica or calcium carbonate) may be worth exploring further, as it has been observed that some coatings undergo partial degradation during the SMD II process. As a result, secretion residue may be damaged by the chemical solubilization of the support layer if they failed to penetrate deeper into the substrate.

Keywords

- Forensic Science
- Chemical analysis
- Porous substrate
- Surface properties
- Gold Nanoparticles

Highlights

- Physical surface topography (roughness and porosity) as well as cellulose and lignin chemical groups have no detectable influence on fingermarks detection using the SMDII technique
- The only factor that may be of importance seems to be the chemical composition of surface coating (silicates and carbonates).

1. Introduction

1.1. Detection of fingermarks using single-metal deposition (SMDII)

Multimetal deposition (MMD) is a fingermark detection technique based on the use of colloidal gold. The application protocol is built along a two-step process: (i) a detection bath containing gold nanoparticles which bind to secretion residue under specific conditions, followed by (ii) a contrast reinforcement bath based on the selective reduction of metal on gold nanoparticles. As a result, MMD-processed fingermarks appear as dark/light-grey ridges on a relatively unstained substrate [1]. Initially named “The Universal Process” [2] for its ability to detect marks on a wide range of substrates (e.g., porous, non-porous, semi-porous, adhesives), the technique was proposed in 1989 [3] and has consistently been improved since, to make it more reliable and user-friendly.

Amongst the various improvements, it is possible to cite the optimization of the colloidal gold synthesis, by Schnetz, to obtain more homogenous (in size and shape) and smaller (from 30 to 14 nm) nanoparticles [4]. This led to MMD II. Another improvement of the technique consisted in replacing the silver-on-gold reinforcement step by a gold-on-gold one [5,6], that proved to produce the same quality of results, with more reliable outcomes, improved control and cheaper costs. At this stage of development, the technique was renamed Single-Metal Deposition (SMD). Finally, the colloidal gold synthesis was further optimized, as well as the application protocol to make it more end-user friendly [7,8]. The latest evolution of the technique, SMD II [8], is characterized by a modified colloidal gold synthesis and a simplified application protocol (e.g., no pH monitoring). As a result, the gold deposition process is more reliable and less pH dependent.

The key step of the technique (being MMD or SMD) remains the gold nanoparticles deposition onto fingermark residue, which is not yet fully understood despite the various optimization and improvement steps. This is a major limiting factor as it makes it difficult to cope with apparent unreliability when processing items or substrates. For example, the technique can give very good results on problematic substrates, such as cling films [9], but suffers from several issues on conventional substrates, such as paper [10]. Among the lack of reproducibility and inconsistent detection performance observed on papers, it is possible to cite: unexplained background staining that can diminish the contrast, unwanted deposition of

gold nanoparticles on the substrate instead of the ridges (reversed detection), or absence of detection (null result). In order to fix those issues, a better understanding of the influence papers may have on the SMD performance is consequently required.

The main objective of this study is to monitor the effect of the composition and structure of different types of paper from North American and European markets on the detection efficiency of SMD II. Spectrophotometric methods as well as paper physics properties (surface pH, surface profilometry, roughness and porosity) were considered to identify the parameters that may influence the quality of the detected fingermarks or induce unwanted background staining. Such knowledge would help designing a more robust and efficient SMD formulation, so that it can be reliable independently from the types of papers. Readers interested in fingermark composition and detection can refer to the most recent publications in the field, such as [11].

1.2. Paper composition and properties

1.2.1 Paper chemical composition

Wood represents the major raw material in the manufacture of paper, aside for specialty papers using cotton or linen, or low grade papers using annual plants. The main constituents of wood are cellulose, hemicelluloses and lignin (Figure 1). Other components, known under the general term of extractives, are present in small and variable quantities. Two types of wood can be distinguished: softwoods (coniferous) and hardwoods, differing mostly by their content in lignin (*i.e.*, 25-35% and 18-25%, respectively). It can be noted that the lignin content in tropical hardwoods may exceed that of many softwoods. Softwoods and hardwoods share a similar amount of cellulose (40-50%), and varying structures and quantities of hemicellulose [12].

< Insert Figure 1 here >

1.2.2 Cellulose

Cellulose is a polysaccharide consisting of a linear chain of several hundreds to many thousands of β(1→4) linked D-glucose units. The cellulose macromolecules are organized in a unit called an elemental microfibril (10 nm in width and 5 nm in thickness), in which there

are about 100 cellulosic polymers connected by intra- and inter-molecular hydrogen bonds. The main characteristic of this polymer is its insolubility in water, which is the result of the very high molecular mass (3000 glucose units).

1.2.3 Hemicelluloses

Hemicelluloses differ from cellulose by the degree of polymerization (150-200), and by the branching of molecular chains (Figure 1, lower right). The constitutive sugars of hemicelluloses are divided into four groups: pentoses, hexoses, hexuronic acids and deoxyhexoses. These units are connected by (1→4) or (1→6) links [12].

1.2.4 Lignin

Lignin is a thermosetting polymer with a very strong aromatic character and a molecular weight that may exceed 40,000 $g.mol^{-1}$. The main constituting unit is the phenylpropane, linked by ether-carbon or carbon-carbon bonds [12]. Lignin ensures the cohesion of the fibers between each other by acting as natural glue. The complexity of lignin is such that much research is still under way to define its molecular structure in a much more precise way. Figure 1 shows a model of the chemical structure of softwood lignin at the top of the figure. Different wood species have different lignin structure and composition.

1.2.5 Surface roughness

Paper roughness is an important parameter for its physical characterization. It is therefore essential to be able to quantify the roughness of a paper so that the given value correlates with the expected use of this paper, for example printing. In our case, it would be interesting to see if surface roughness can be correlated with the quality of affixing of the secretion residue composing the fingermarks on the different types of paper.

Roughness is defined as the average distance between the paper surface and a reference plane to be defined. The roughness indices increase with the roughness of the paper [13]. Various parameters such as Ra, Rq, Rt and Rz are defined to quantify the roughness of a paper surface (Table 1). Rq is the value we will use in our analysis.

< Insert Table 1 here >

1.2.5 Porosity

Paper has a porous structure formed by a network of fibers. Accordingly, there is a two-phase arrangement in which pores and voids between fibers form an important part of its structure [14]. Paper porosity is correlated with several properties such as absorption, opacity, and ink-paper interaction. The porosity is influenced by the processing conditions, the addition of pigments and chemical additives. For some grades of paper, a coating is applied to the top surface of the paper to change its porosity [15].

In forensic science, an appropriate fingermark detection sequence is usually chosen by associating the item to one of the main substrate classes: porous, non-porous or semi-porous (if we exclude specific substrates such as adhesives, metals, etc.). These categories are based on the apparent (empiric) porosity of the substrate, which is known to influence the behavior of the secretion residue [11]. Office papers are associated with porous substrates, while magazine papers are usually considered as semi-porous substrates.

2. Material and Methods

2.1. Paper collection and characterization

2.1.1 Paper sampling

74 different kinds of paper (e.g., inkjet, LaserJet, copier, envelope, newsprint, Offset, drawing, artistic) from 70 to 275 $g.m^{-2}$ basis weight were used in this study (see Appendix A for details). These paper samples originated from Europe (*e.g.*, Germany, Austria, Finland, France, Portugal, Sweden and Switzerland), Canada, Mexico, and United States of America. The samples were characterized by a range of paper composition: sugar cane (95%), cardboard, colored, recycled fibers (10, 20, 30, 50% and even 80% post-consumer fibers), wheat, FSC (Forest Stewardship Council) approved, Kraft, bleached Kraft, bleached generic and blended mixed FSC.

2.1.2 UV-Visible-NIR spectroscopy

UV-visible spectra were taken on a Varian/Agilent Cary 5000 UV-VIS-NIR spectrophotometer equipped with a diffuse reflectance integrating sphere (350-850 nm for UV-Visible part and 4000-600 cm^{-1} for IR). The choice of this method is necessary because paper is a solid,

strongly absorbent, and highly diffusive material. The main functional groups responsible for the sensitivity to light of lignin are the carbonyl and phenolic groups, quinones and various conjugated double bonds [12].

Ten spectra of each paper sample were recorded, averaged and analyzed using the ACD/SpecManager™ version 12.00 from ACD/Labs (*Advanced Chemistry Development*) software.

2.1.3 Profilometry

3D profiles of the paper surface were recorded with a contact free optical profilometer (Veeco Wyko NT1100™ instrument) using a Mirau interferometer. Phase shift interference (PSI) and vertical offset interference (VSI) can be used to respectively measure smooth and rough surfaces (heights that can reach up to 1mm). Those two modes were used to optimize detection and measurements of the paper samples.

2.1.4 Porosity measurements

Porosity measurements were carried out with a Parker Print Surf™ (PPS) device from Hagerty Technologies™. The flow of a fluid (air in our case) that passes through the paper was measured with a pressure of 1960 kPa.

2.1.5 Surface pH measurements

pH measurements were carried out with a pH Pencil from HYDRION™, measuring a gradient of H_3O^+ ions on the paper surface. The first step was to moisten the surface of the paper with distilled water, then to mark a line with the pen. After 15 minutes, the color of the line was compared with the shades of color (color sheet) accompanying the pen. Although this method is not fully accurate, it is a good way to discriminate a wide range of surface pH otherwise very difficult to measure, and as pH is the most critical parameter to control for SMD development, it could be planned that such an easy semi-quantitative pH tester could be deployed to assist practitioners.

2.2. Fingermark collection

Natural and sebum-rich marks from two donors were collected for this study. For the natural fingermarks, the donors were asked not to wash their hands one hour prior deposition. No intentional enrichment was performed before collecting the fingermarks. For the sebum-rich marks, the donors rubbed their hands on their forehead before depositing the fingermarks. One natural and one sebaceous-rich marks were collected in duplicate for each donor and substrate. Fingermarks were left to age for one month in the dark. This aging period has been chosen to avoid the processing of fresh marks (e.g., one-day-old or one-week-old marks) and to focus on marks compatible with a casework timeline. Temperature and humidity were not monitored, nor controlled.

2.3. Fingermark detection, quality rating and background evaluation

The paper samples bearing fingermarks were processed using the latest SMD II protocol [8]. . Given that paper can modify the pH of the solution and have an adverse impact on the results, the paper samples were cut so that they all weight the same mass. Each paper sample was then processed in 200 ml of colloidal gold solution. Since the focus of the study is to investigate the effect of the different types of paper on the SMD II performance, each paper type was processed in a newly prepared bath of colloidal gold. After completion of the SMD II protocol, the samples were left to dry before being scanned on an Epson Perfection V330 Photo™ at 1200 dpi, without any digital enhancement. Once scanned, each mark was rated by three independent assessors using a scale ranging from 0 to 3 (Table 2 [16]).

SMD II is known to produce unwanted, uncontrolled and non-homogeneous darkening of the porous substrate. In order to understand what parameters may trigger background staining, the color of each paper was recorded before and after fingermark detection. Background measurement was done as follows: for each paper type, an unprocessed sample was placed next to a processed sample and photographed under a homogeneous lighting. Photographs were taken in grey scale and the value of the color was extracted using the eyedropper tool on Adobe Photoshop. Those values range from 0 (black) to 255 (white). For unprocessed samples, one measurement was made in the center of the paper. Processed samples required to conduct four measurements at four different locations which were then averaged, to take background staining inhomogeneity into account. The obtained value was then subtracted from the value of the unprocessed sample. A positive value means a darkening of the substrate whereas a negative value means a lightening.

< Insert Table 2 here >

2.4. Statistical Analysis

In order to highlight the potential correlation between the results of SMD II and the different analyses performed on paper samples, a data analysis was performed. As a first step, the raw results were organized using a Microsoft Office Excel spreadsheet. The analytical part was performed with the data processing software "R 3.0.2". The different methods of analysis considered were (i) the chi-square test where each variable extracted from the paper analyses was assessed against the results of SMD II (fingermark quality and background staining) and (ii) a joint analysis of variables using principal component analysis (PCA), multiple correspondence analysis (MCA) and multiple linear regression (MLR).

3. Results and Discussion

3.1 Paper characterization (before SMD II)

3.1.1 UV-Visible spectroscopy

Figure 2 shows the processing of the UV-Visible spectrum obtained for the sample “C03”. Each processed spectrum represents the variation of the log of the inverse of the reflectance as a function of wavelength.

< Insert Figure 2 here >

Figure 3 shows the UV-Visible spectra of some North American (C01 and C02) and European (E21 and E31) samples. The spectra show absorptions in the UV-Visible region. These absorptions are due to the presence of lignin and the colored products of the paper (dyes, coating pigments).

< Insert Figure 3 here >

It is possible to deconvolute the spectra to identify the electronic transitions between the various occupied molecular orbitals (OMO) and unoccupied molecular orbitals (UMO), if these are involved in our study.

The 100 to 350 nm region has not been considered because of the intense background noise cause by the presence of even a small amount of lignin. UV-Visible analysis of SMD II-processed samples shows an increase in absorption for some of the papers and a decrease for others.

The reduction in the intensity of absorption of the spectral bands can be explained by 1) the oxidation of the chromophores during the SMD II process. This has led to the displacement of the other bands at longer wavelengths, towards the red part of the spectra (bathochromic effect) and 2) the breaking the double bonds and formation of new compounds by modification of polarity. Other papers are characterized by hypochromic displacements to shorter wavelengths (towards ultraviolet).

3.1.2 IR spectroscopy

The four most important infrared regions for cellulose are the region of the bound and free OH elongations between 3660 and 3000 cm^{-1}, the region of the aliphatic CH elongations between 3000 and 2800 cm^{-1}, the region of elongations C-O alcohols (or a cyclic system) of between 1350 and 1000 cm^{-1}, as shown in Table 3.

IR analysis showed that the many bleached papers samples designed for printing purpose contain very small amounts of lignin. We also observed that about 80% of the samples (apart from photographic papers and some colored papers) possess a carbonate coating, mainly because these papers are intended for printing.

Carbonate characteristic peaks are located between 2530-2500, 1815-1770, and 1490-1370 cm^{-1} (CO_3^{2-} elongation band), 910-850 cm^{-1} (O-C-O deformation band), 885-870 cm^{-1} and 715 cm^{-1} [17]. FTIR analysis of a calcium carbonate powder allowed the identification of these bands and with the use of the ACD/SpecManager software, identification of these bands in the paper samples was possible. This allowed subsequent verification of the presence or loss of the carbonate layer after treatment with the SMDII.

< Insert Table 3 here >

3.1.3 Profilometry and roughness

The profilometry allowed obtaining the 3D topography of all paper samples (Figure 4). For sample C01, which is a glossy white paper used for inkjet printing, a uniform surface has been measured, with very low Rq (0.068±0.009µm). This makes sense given that the surface is coated with a layer of mineral pigments which makes the surface of this paper smoother and brighter.

< Insert Figure 4 here >

Figure 5 shows the value and variation of the Rq values of North American and European papers. The parameters Ra, Rq, Rt and Rz characterizing the roughness of each paper give the same variation, whether for North American or European papers. Rq corresponds to the quadratic mean value of the profile deviations. Rq values ranged from 0.07±0.01 µm to 6.07±0.01 µm for papers from North America and from 3.1±0.6µm to 4.5 ± 1.1µm for samples from Europe. The standard deviations of the different measurements are high (Figure 5), because the samples are not uniform at the microscopic level.

< Insert Figure 5 here >

3.1.4 Porosity

Figure 6 shows the variation in average airflow in mL/min of North American and European samples. It can be noted that there is a very large variation in air flow, which makes it possible to distinguish the most porous samples from less porous ones.

< Insert Figure 6 here >

We have attempted to find a relationship between surface roughness and porosity (Figure 7). This analysis is presented as the variation of Rq as a function of the airflow rate. Our results indicate that roughness and porosity of the paper are not correlated

< Insert Figure 7 here >

3.1.5. Surface pH

The values of surface pH reported for the tested paper samples can be found in Appendix A. The majority of the tested papers have a neutral pH (82%), while only a few have a slightly acidic (10%) or basic pH (3%). This result was expected since most of writing papers are

acid-free for document preservation purposes. Only three paper types have a pH of 4 or 5 (C01, C20, C41).

3.2 Impact of SMD II on the paper properties

3.2.1 Carbonate-coated papers

The IR spectra of carbonate-coated samples before and after the application of SMD II were mathematically subtracted from each other and compared with the spectrum of calcium carbonate. Figure 8 illustrates the results obtained for the paper sample RetroPlus50 Canada (C02). It appears that the loss observed on the spectrum resulting from the subtraction “after-before SMD II” (Figure 8 - top) could be correlated with the loss of calcium carbonate (Figure 8 - bottom).

< Insert Figure 8 here >

This loss can be explained by the fact that SMD II requires to immerse the papers in an acidic solution (pH close to 3). IR analysis allows identifying the peaks of the different components and hence estimate a loss of carbonate. However, the quantitative analysis must be completed with chemical analysis to confirm the proportions of carbonates present. When assessing the % of loss by looking at the carbonate absorption band, it appears that most of the paper samples loose between 20 to 50% of this layer. Some papers undergo a total loss (100%). One hypothesis could be that the detrimental effect that SMD II has on the carbonate layer do have a direct impact on the detection performance. This hypothesis will be investigated further in this contribution.

3.2.2 Photographic papers

It was not easy to determine the exact composition of the photographic papers with the IR analyzes. Figure 9 shows the three IR spectra of the sample C01, the first spectrum at the top shows the result of the subtraction between the spectra recorded before and after SMD II was applied. What can be seen on this difference spectrum is that there is a loss of three bands which are at 1721, 1653 and 1423 cm^{-1} and a band amplification at 1584 cm^{-1} which is identifiable in the post-SMD II spectrum.

< Insert Figure 9 here >

The subtraction between the pre-SMD II spectrum of C01 and another sample, for example C04 (for which we were able to determine its cellulose and carbonate composition) shows that no peak corresponds to cellulose in the C01 spectrum, as shown in Figure 10. The photographic coating layer is probably too thick for the infrared radiation to reach the inner layers of the paper. All the photographic papers collected in this study are also coated with silicate, as shown in our FTIR spectra.

< Insert Figure 10 here >

Silicate in its various forms (gel, precipitate or colloidal) is the most widely used pigment for the coating of photographic paper to provide a smooth and shiny surface [18]. The most characteristic peaks of silicate are shown in Table 4 [19,20,21]. All photographic samples considered in this study have a silicate coating. The positions of the spectral bands depends on the type of silica used, as well as on the way the coating recipe is prepared (temperature, solvent used, etc.).

< Insert Table 4 here >

Post-SMD II IR analysis showed that there was no change at the surface of the photographic paper, and therefore no loss of this layer. This can be explained by the fact that the silica layer is quite thick and that it remains stable at acidic pH (no dissolution of this layer). In reference [18], the author describes the factors influencing the dissolution of amorphous silica. Among these factors, the pH has a limited role as the dissolution is almost negligible for pH below 3 and above 9. Finally, the infrared analysis did not allow the determination of the type (or composition) of silica used for the coating of the photographic papers considered in this study.

3.2.3 Colored papers

Some colored papers are coated with carbonate (C03, C08, C32, E30, E31, E32), while others contain very little or no carbonate, such as C23 and C27 (all colors), E27, E28 and E29. For the sample C27, IR analysis shows the presence of cellulose (Figure 11). The other peaks belong to the aromatic compounds present (CH aromatic elongation 3083, 3060, 3026 cm^{-1}, elongation C=O 1730 and 1704 cm^{-1}, CC elongation of the aromatic ring at 1601, 1493, 1452 cm^{-1}, out-of-plane deformation CH aromatic at 697 cm^{-1}).

For the post-SMD II IR spectrum for sample C23 (with all colors), the intensity of certain bands (1468 and 1445 and 853 cm^{-1}) decreased, while the intensity of other bands increased (1731, 1155 cm^{-1}). The difference between the spectra obtained before and after SMD II emphasizes this decrease but no loss of spectral bands. This is also true for sample C27.

< Insert Figure 11 here >

Several paper samples (C10, C33, C37, C40, E08, E11, E16, E18, E19, E20, E21, E22, E27 E28, E29 E31, E30, E32) showed spectral band losses at 3340-3350 cm^{-1} and at 2920 cm^{-1}. Probably it is the CH_2-OH group of the cellulose which is lost during the treatment with SMD II (protonation of the alcohol in an acidic medium). The calculation of the derivative with the ACD/SpecManager software made it possible to identify the IR bands corresponding to the carbonate and the cellulose. The band at 711 cm^{-1} is identified in the carbonate with an accuracy of ±1 cm^{-1}. This band is used to calculate the amount of carbonate lost during the processing with SMD II (this band is easily identifiable) (Figure 12).

< Insert Figure 12 here >

3.4 Correlation between the SMD II performance and the paper characteristics

Overall, 592 fingermark samples were processed and assessed throughout the study, leading to fingermarks detected with scores ranging from 0 to 3. As expected, the technique also led to background noise inducing a darkening of the paper surface for most paper types. The colored papers presented a lightening of the color, most certainly due to the successive water baths of the SMD II protocol.

The quality scores that have been associated with the detected fingermarks are representative of the performance of SMD II on each paper sample. To some extent, the fact that the same donors provided natural marks along the study makes it possible to compare all these scores and try figuring out some trends among the paper samples. Different correlations with the detection quality scores were explored: *vs* porosity (Figure 13), *vs* surface roughness (Figure 14), *vs* surface pH (Figure 15), and *vs* amount of carbonate lost (Figure 16). It was indeed supposed that characteristics such as the paper porosity, the surface roughness or the surface pH would play a direct role in the way SMD II behave (detection quality and background). Also, given that a loss of calcium carbonate has been

observed, it appeared interesting to see if the modification of this layer may be correlated with the SMD II performance.

< Insert Figure 13 here >

< Insert Figure 14 here >

< Insert Figure 15 here >

< Insert Figure 16 here >

When focusing on papers presenting no apparent issues in regards to fingermark detection (quality scores close to 3), it can be seen that the porosity is rather low, with average airflow ranging from 0 to 1000 mL/min, the roughness is characterized by Rq values ranging from ca. 3 to 4 microns, the surface pH of the paper ranges from 4 to 7 and the loss of carbonate ranges from ca. 30% to ca. 90%. However, papers leading to bad quality fingermarks (quality scores close to 0) also present similar characteristics; their porosity is low to average, with average airflow ranging from 0 to 1500 mL/min, the roughness is characterized by Rq values ranging from ca. 2.5 to 4 microns, the surface pH ranges from 6 to 7, and the loss of carbonate ranges from ca. 10% to 100%.

Therefore, from the analysis of Figures 13 to 15, no clear trends can be identified regarding the quality of fingermarks in regards to porosity, surface roughness or surface pH of the papers analyzed. The same observation is made with the loss of calcium carbonate.

About the surface pH, it can be noted that papers with acidic surface pH (below 6) led to no zero quality scores, which means that SMD II was able to detect fingermarks for each of them, but with varying quality levels. Beyond that observation, there seems to be no trend between surface pH and SMD II performance. 85% of the paper samples are indeed characterized by surface pH between 6 and 7, with quality scores ranging from 0 to 3. Contrarily to what could be expected, an acidic surface pH is consequently not necessarily associated with better detection quality.

From the analysis of some 3D topographies of the different types of samples, it is remarkable that the same type of surface does not give the same quality of revelation of the fingermarks,

as it is for the C02 samples (quality score of 0.67) and C05 (quality score of 1.84). Illustrations of processed paper samples bearing fingermarks are shown in Appendix B.

To further refine the analysis, statistical analysis was used to try and detect correlation between background noise, fingermark quality and the paper variables. However, none of the techniques used (Chi-square test, PCA, MCA and MLR) led to the detection of a correlation between the parameters considered.

3.5 General discussion

Despite the number of different paper types collected, the various paper properties studied and the large number of fingermarks processed with SMD II, no correlation between paper properties and SMD II efficiency was highlighted. However, the chemical composition of the surface coating is worth discussing further.

Regarding the experimental design, the number of donors has been voluntarily set low because the study had not for aim to assess the intrinsic performance of SMD II as fingermark detection technique. It rather aimed at studying the influence of paper samples on its ability to detect fingermarks. Doing so requires limiting other influencing parameters, such as the variability induced by donors and the age of the fingermarks. By choosing two average donors, it was possible to assess how the performance of SMD II evolves when different paper samples are considered. Increasing the number of donors would have not modified the overall conclusions of the study and would have imply reducing the number of paper samples to keep the quantity of fingermarks manageable.

Surface coating is made of silica or calcium carbonate. It is used to make the surface uniform and improve the printing quality [22]. This coating is however soluble in acidic aqueous solutions. Therefore, immersing the samples in colloidal gold will lead to its partial dissolution. If the fingermark residue does not migrate deep enough in the layer of the paper [23], it will be damaged. The dissolution of the fingermark may rely on two parameters: the thickness of the coating layer and the depth of penetration in the paper. According to Vallette and Choudens [22], and Santos et al. [24], the thickness of the coating is about 15 µm for paper of a weight of 72 g/m^2 and more. It is also known that penetration depth depends on the paper type [23]. On coated papers, observed depth could be as deep as 30 µm. It means that even if the layer

is entirely removed, a fraction of the fingermark residue may remain available for detection. Uncoated papers contain calcium carbonate as well to improve their surface characteristics and whiteness. This material may also be solubilised during SMD II processing and lead to fingermark degradation. Under these circumstances, the dynamic of diffusion of the secretion residue into the substrates is expected to play a major role. Indeed, it could be hypothesized that if the secretion residue has not migrated through the surface coating when the document is processed by SMD II, its chance of being detected would be seriously reduced. The key parameter to consider in a forthcoming study will be the aging time of the fingermarks, as we made the choice to limit our study to one-month-old fingermarks for experimental reasons. This observation is also compatible with another technique known to interact with the non-water-soluble fraction of the secretion residue, that is, physical developer (PD). Previous studies have shown that the performance of PD increases with the age of fingermarks [25]. Moreover, this technique requires an acid pre-treatment to neutralize the alkali filler particles and to avoid an overall staining of the item. This appears compatible with the need for secretion residue to penetrate the substrate beyond the filler/coating layers to have a chance to be detected. Consequently, it may be interesting to correlate such conclusions with the results of the present study, based on SMD II.

4. Conclusions

This study aimed at characterizing several paper types (e.g., surface composition, surface pH, roughness and porosity) before and after the application of SMD II. Furthermore, we investigated the possibility to correlate the measured parameters with the performance of SMD II, in terms of ridge quality and background staining.

At the completion of this study, we were able to show that the following parameters show no correlation with the SMD II performance: paper roughness, porosity and surface pH. IR analysis showed that 81% of the papers are coated with carbonates and the thickness of this layer varies from one sample to another. This layer appears to be solubilized during the SMD II process. Since fingermarks are originally present at the surface of this coating, further investigation should be carried out considering the correlation between the calcium carbonate thickness and the SMD II detection performance. One hypothesis is that secretion residue may migrate below the calcium carbonate layer if it is not too thick, and be further detected by SMD II despite the dissolution of the carbonate-based coating. This hypothesis is worth being

further studied considering fingermarks of different ages. Moreover, it is expected that these observations will be useful to physical developer as well.

Table 1

Parameter	Description	Formula
Ra	Arithmetic mean of absolute values of deviations *y*	$R_a = \frac{1}{n}\sum_{i=1}^{n}\lvert y_i \rvert$
Rq	Quadratic mean value of the profile deviations	$R_q = \sqrt{\frac{1}{n}\sum_{i=1}^{n}\lvert y_i \rvert^2}$
Rt	Maximum Profile Height	$R_t = R_p - R_v$
Rz	The mean height difference between the 5 highest peaks and the 5 lowest valleys	$R_z = \frac{1}{5}\sum_{i=1}^{5} R_{pi} - R_{vi}$

Table 2

Score	Qualitative observation
0	No ridge, no fingermark visible
1	Ridges are visible over a small area (or over the whole mark), but it is extremely difficult to retrieve level II characteristics (such as minutiae) due to extremely poor ridge details.
2	Ridges are visible on almost the whole mark; level II characteristics can be retrieved. Nevertheless, the quality is not optimal due to a low contrast, strong background staining or faint ridges.
3	Ridges are very well defined on the whole mark. Level II characteristics can easily be retrieved. The contrast is optimal with no (or extremely faint) background staining.

Table 3

Frequency (cm^{-1})	Attribution
3332	O-H elongation with intramolecular
2897	CH_2
1634	H_2O
1426	CH_2 symmetrical deformation
1370	C-H deformation
1334	C-H shear (plane)
1316	CH_2 agitation
1281	C-H deformation
1203	O-H deformation
1160	C-O and C-C elongation + CH_2 rocking
1105	C-O and C-C elongation + CH_2 rocking
1052	C-O elongation
1029	C-O elongation
1002	C-O and C-C elongation + CH_2 rocking
897	Out-of-plane O-H deformation
659	Out-of-plane O-H deformation

Table 4

Frequency (cm^{-1})	Attribution
3700-3200	Si-OH
3360	H_2O absorbed
3000-2800	Organic C-H
1733, 1653, 1634	H_2O absorbed
1423	CH_2 symmetrical deformation
1870-960	Vibrational network SiO_2
1350-500	C-H vibration
1070	Si-O-Si symmetrical elongation
900-980	Free silanol elongation
800-820	Si-O-Si symmetrical elongation

Figure captions

Figure 1 Chemical structures of the major wood components: lignin (top), cellulose (bottom left), and hemicellulose (bottom right) [12]

Figure 2 Example of treatment of the UV-Visible spectrum, from % Reflectance to log of inverse reflectance allowing spectrum deconvolution, for the Staples Pastel (USA, CO3). Red vertical line is λ_{max}, blue line is actual spectrum, green curves are the resulting deconvoluted bands representing electronic transitions, and black spectrum represent the result of the fitted deconvolution.

Figure 3 UV-Visible spectra of some of the analyzed paper samples. a) Kirkland Signature (Mexico, C01), b) RetroPlus50 (Canada, C02), c) Esquisse envelope (France, E21), d) Papyrus rainbow (Europe – unspecified country, E31).

Figure 4 Left half: 3D profiles of the RetroPlus50 (Canada; C02) and Staples Sustainable Earth Copy Paper (USA; C05) paper samples after they were processed with SMD II. Right half: illustration of the processed samples.

Figure 5 Average values of the Rq parameter (µm) for all the paper samples (see Appendix A for manufacturer details).

Figure 6 Average air flow (mL/min) measured for all the paper samples (see Appendix A for manufacturer details).

Figure 7 Chart illustrating the relation between the average airflow (mL/min) and the Rq values (microns) for all the paper samples. Each dot represents a paper sample.

Figure 8 Top spectrum resulting from the subtraction of the IR spectra obtained before and after the application of SMD II on the paper sample RetroPlus50 Canada (C02); bottom IR spectrum corresponding to calcium carbonate.

Figure 9 Top spectrum obtained by subtracting the IR spectra obtained before (middle) and after (bottom) the application of SMD II (paper sample: Kirkland Signature Mexico; C01).

Figure 10 Difference spectra between C04 (top) and original C01 (bottom).

Figure 11 Infrared spectrum of the unprocessed Staples "Chemise à pochettes – 1336" paper sample (C27).

Figure 12 Derivative calculation for the RetroPlus50 paper sample (Canada; C02). Top spectra represent the paper surface with the fingermarks revealed, while bottom spectra represent the opposite surface of the same paper.

Figure 13 Chart illustrating the relation between the airflow (mL/min) and the average quality score associated with the fingermarks obtained after SMD II. Each dot represents a paper sample.

Figure 14 Chart illustrating the relation between the Rq values (microns) and the average quality score associated with the fingermarks obtained after SMD II. Each dot represents a paper sample.

Figure 15 Chart illustrating the relation between the surface pH and the average quality score associated with the fingermarks obtained after SMD II. Each dot represents a paper sample.

Figure 16 Chart illustrating the relation between the calcium carbonate loss (estimated %) and the average quality score associated with the fingermarks obtained after SMD II. Each dot represents a paper sample.

Table captions

Table 1 Parameters Ra, Rq et Rz used to qualify paper surface roughness (n being the number of peaks of the profile).

Table 2 Table used to assess the quality of the marks (reproduced from [16]).

Table 3 Main infrared peaks characteristic of cellulose in the majority of papers studied [**Error! Bookmark not defined.**].

Table 4 The main infrared peaks characteristic of the silicate gel [19,20,21]

Competing statement

The authors declare that they do not have any competing interest to declare.

Funding

The authors thank NSERC (National Sciences and Engineering Research Council of Canada), FRQNT (Fonds de Recherche du Québec – Nature et Technologies) and CQMF (Centre Québécois sur les matériaux fonctionnels, Gouvernement du Québec) for financial support.

References

1 A. Bécue, S. Moret, C. Champod, P. Margot, Use of stains to detect fingermarks. Biotech. Histochem, **86**:3 (2011) 140-160. https://doi.org/10.3109/10520290903462838.

2 G.C. Saunders, A.A. Cantu, Universal Process for Fingerprint Detection. Los Alamos National Laboratory Publication, **April** (1991).

3 G.C. Saunders, Multimetal deposition method for latent fingerprint development. in 74th annual educational conference of the International Association for Identification. (1989). Pensacola, FL.

4 B. Schnetz, P. Margot, Technical note: latent fingermarks, colloidal gold and multimetal deposition (MMD) - Optimisation of the method. Forensic Sci. Int., **118**:1 (2001) 21-28. https://doi.org/10.1016/S0379-0738(00)00361-3.

5 E. Stauffer, A. Bécue, K.V. Singh, K.R. Thampi, C. Champod, P. Margot, Single-metal deposition (SMD) as a latent fingermark enhancement technique: An alternative to multimetal deposition (MMD). Forensic Sci. Int., **168**:1 (2007) e5-e9. https://doi.org/10.1016/j.forsciint.2006.12.009.

6 P. Durussel, E. Stauffer, A. Bécue, C. Champod, and P. Margot, Single-Metal Deposition: Optimization of this Fingermark Enhancement Technique. J. For. Ident., 2009. **59**(1): p. 80-96. https://doi.org/10.1016/j.forsciint.2006.12.009.

7 A. Bécue, A. Scoundrianos, S. Moret, Detection of Fingermarks by Colloidal Gold (MMD/SMD) - Beyond the pH 3 Limit. Forensic Sci. Int., **219:**1-3 (2012) 39-49. https://doi.org/10.1016/j.forsciint.2011.11.024.

8 S. Moret, A. Bécue, Single-Metal Deposition for Fingermark Detection - A Simpler and More Efficient Protocol. J. For. Ident., **65**:2 (2015) 118-137.

9 C. Fairley, S.M. Bleay, V.G. Sears, N. Nic Daéid, A Comparison of Multi-metal Deposition Processes Utilising Gold Nanoparticles and an Evaluation of their Application to "Low Yield" Surfaces for Finger Mark Development. Forensic Sci. Int., **217**:1-3 (2012) 5-18. https://doi.org/10.1016/j.forsciint.2011.09.018.

10 T.G. Newland, S. Moret, A. Bécue, S.W. Lewis, Further investigations into the single metal deposition (SMD II) technique for the detection of latent fingermarks. Forensic Sci. Int., **268** (2016) 62-72. https://doi.org/10.1016/j.forsciint.2016.09.004.

11 C. Champod, C. Lennard, P. Margot, M. Stoilovic, Fingerprints and Other Ridge Skin Impressions - Second Edition. (2016), Boca Raton, Florida: CRC Press LLC. 427. ISBN 9781498728935.

12 D.N.-S. Hon, N. Shiraishi, Wood and Cellulosic Chemistry, Second Edition, Revised, and Expanded, Marcel Decker Inc, New York, (2000), 928 Pages, ISBN 9780824700249.

13 C. Antoine, Optimisation de l'état de surface des papiers supercalandrés (grade SCA) pour l'impression héliogravure, Master thesis, UQTR, (1996), URL: http://depot-e.uqtr.ca/4657/1/000626161.pdf

14 S. Adanur, Paper Machine Clothing: Key to the Paper Making Process, Technomic Publishing Company Inc., (1997). ISBN 1-56676-544-7.

15 J.W. Martin, Concise Encyclopedia of the Structure of Materials, Elsevier Ltd, (2007). ISBN-10: 0-08-045127-6, ISBN-13: 978-0-08-045127-6.

16 T. Fitzi, R. Fischer, S. Moret, A. Bécue, Fingermark Detection on Thermal Papers: Proposition of an Updated Processing Sequence. J. For. Ident., 64:4 (2014) 329-350.

17 F.A. Miller, C.H. Wilkins, Infrared Spectra and Characteristic Frequencies of Inorganic Ions – Their Use in Qualitative Analysis, Anal. Chem., 24:8 (1952) 1253-1294. https://doi.org/10.1021/ac60068a007.

18 Svanholm, Erik., Printability and Ink-coating Interactions in Inkjet Printing, Karlstad University Studies, (2007). ISBN 91-7063-104-2.

19 G. Socrates, Infrared and Raman Characteristic Group Frequencies Tables and Charts, Third Edition, John Willey & Sons,LTD, New York, (2001). ISBN: 978-0-470-09307-8.

20 R.F.S. Lenza, W.L. Vasconcelos, Preparation of Silica by Sol-Gel Method Using Formamide, Mat. Res., 4:3 (2001). https://doi.org/10.1590/S1516-14392001000300008.

21 A.M. Putz, M. Putz, ,Spectral Inverse Quantum (Spectral-IQ) Method for Modeling Mesoporous Systems: Application on Silica Films by FTIR, Int. J. Mol. Sci. 13 (2012) 15925-15941. https://doi.org/10.3390/ijms131215925.

22 P. Vallette, C. Choudens, Le Bois, la Pâte, le Papier, deuxième édition, Centre Technique de l'Industrie des Papiers, Cartons et Celluloses, 1989.

23 J. Almog, M. Azoury, Y. Elmaliah, L. Berenstein, A. Zaban, "Fingerprint's third dimension: The depth and shape of fingerprints penetration into paper - Cross section examination by fluorescence microscopy", J. Forensic Sci. 2004;49(5):981-985

24 N.F. Santos, J. Velho, C. Gomes, Influence of calcium carbonate coating blends upon paper properties, Congreso iberoamericano de investigacion en celulosa y papel, 2000.

25 J. Salama, S. Aumeer-Donovan, C. Lennard, C. Roux, Evaluation of the fingermark reagent Oil red O as a possible replacement for physical developer, J. For. Ident., 58:2 (2008) 203-237.

Figures

Graphical Abstract (1328 x 531 pixels at 96 dpi)

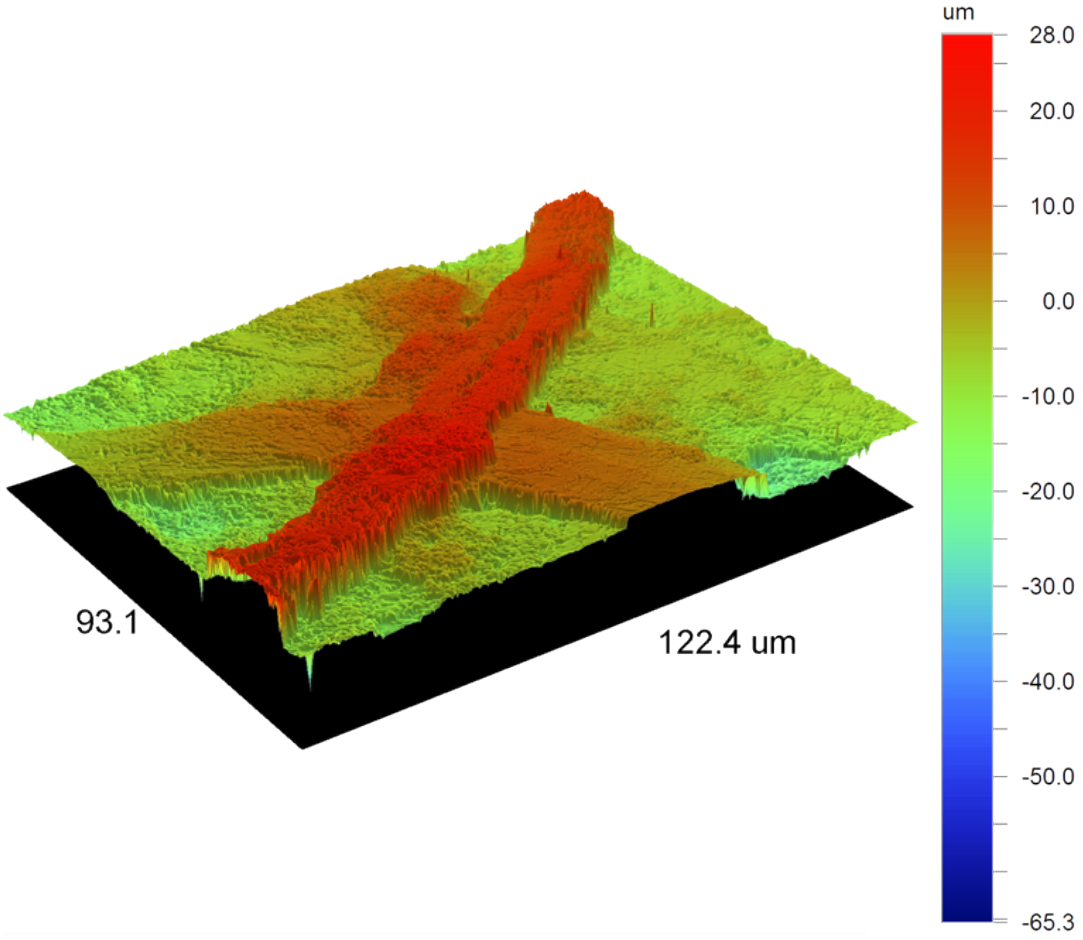

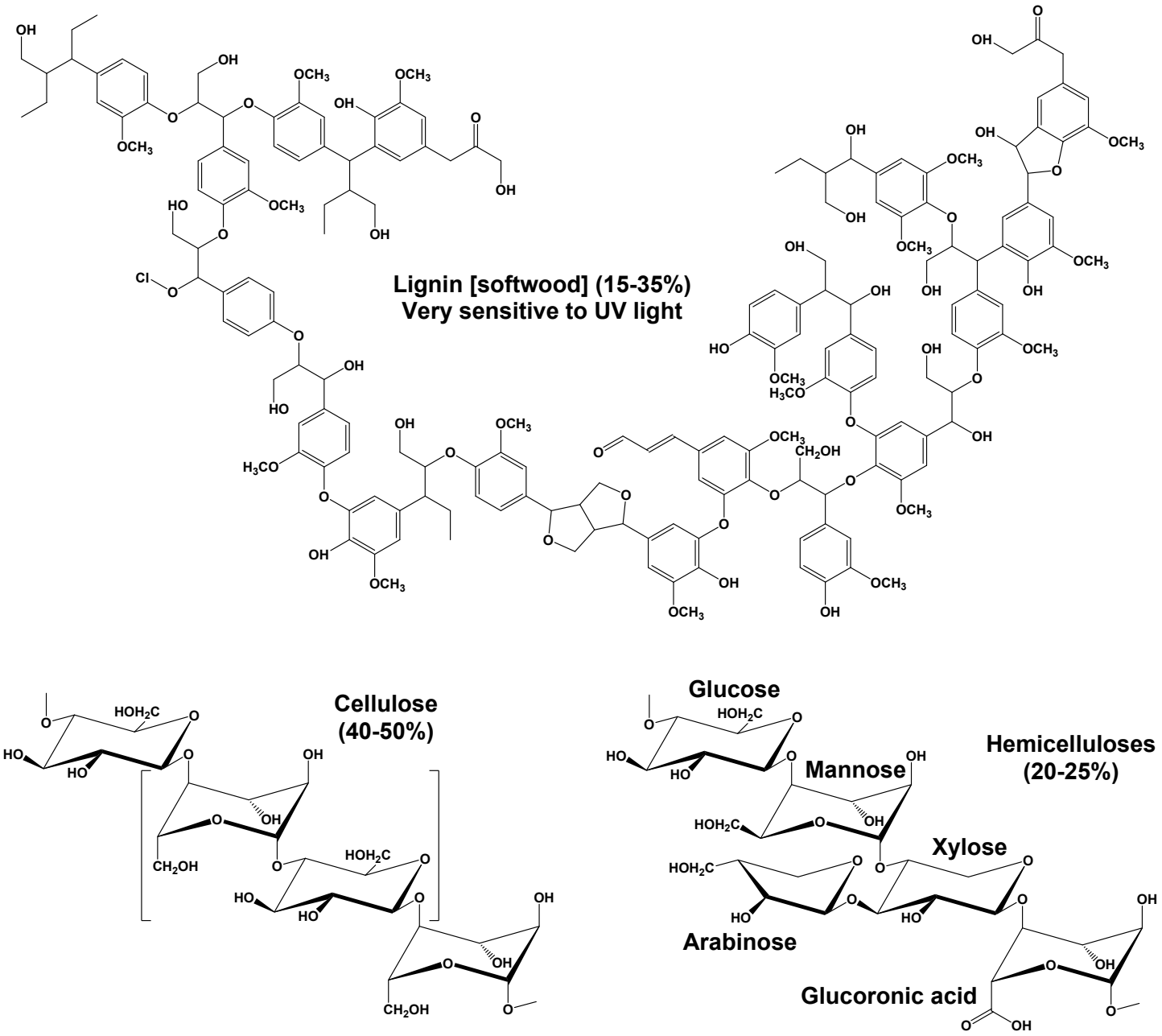

Figure 1 Chemical structures of the major wood components: lignin (top), cellulose (bottom left), and hemicellulose (bottom right) [12]

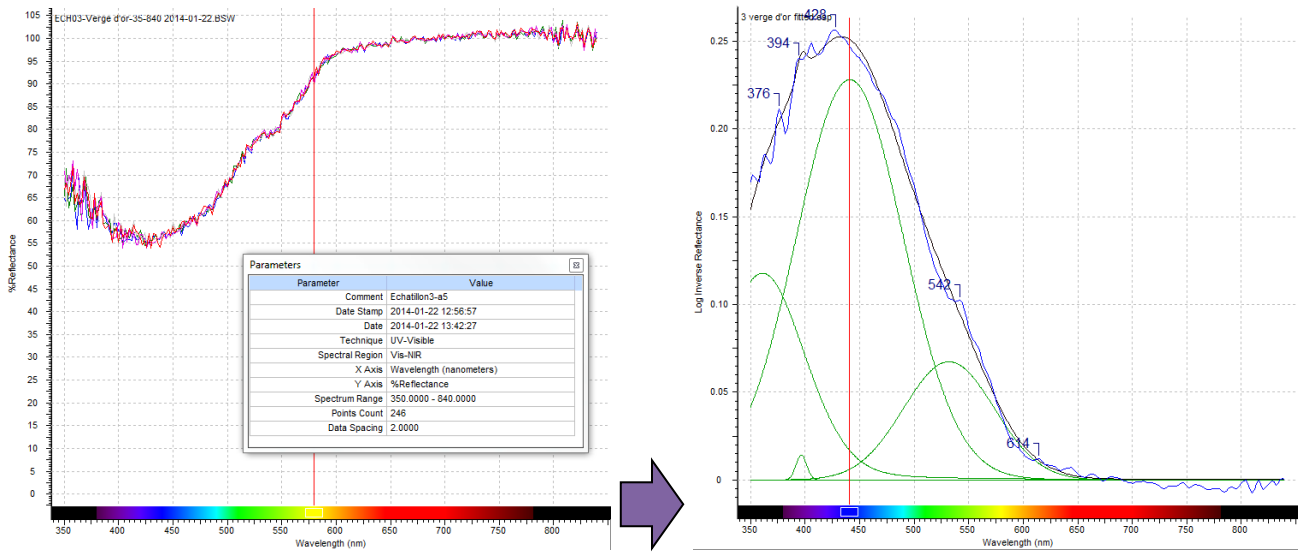

Figure 2 *Example of treatment of the UV-Visible spectrum, from % Reflectance to log of inverse reflectance allowing spectrum deconvolution, for the Staples Pastel (USA, CO3). Red vertical line is λ_{max}, blue line is actual spectrum, green curves are the resulting deconvoluted bands representing electronic transitions, and black spectrum represent the result of the fitted deconvolution.*

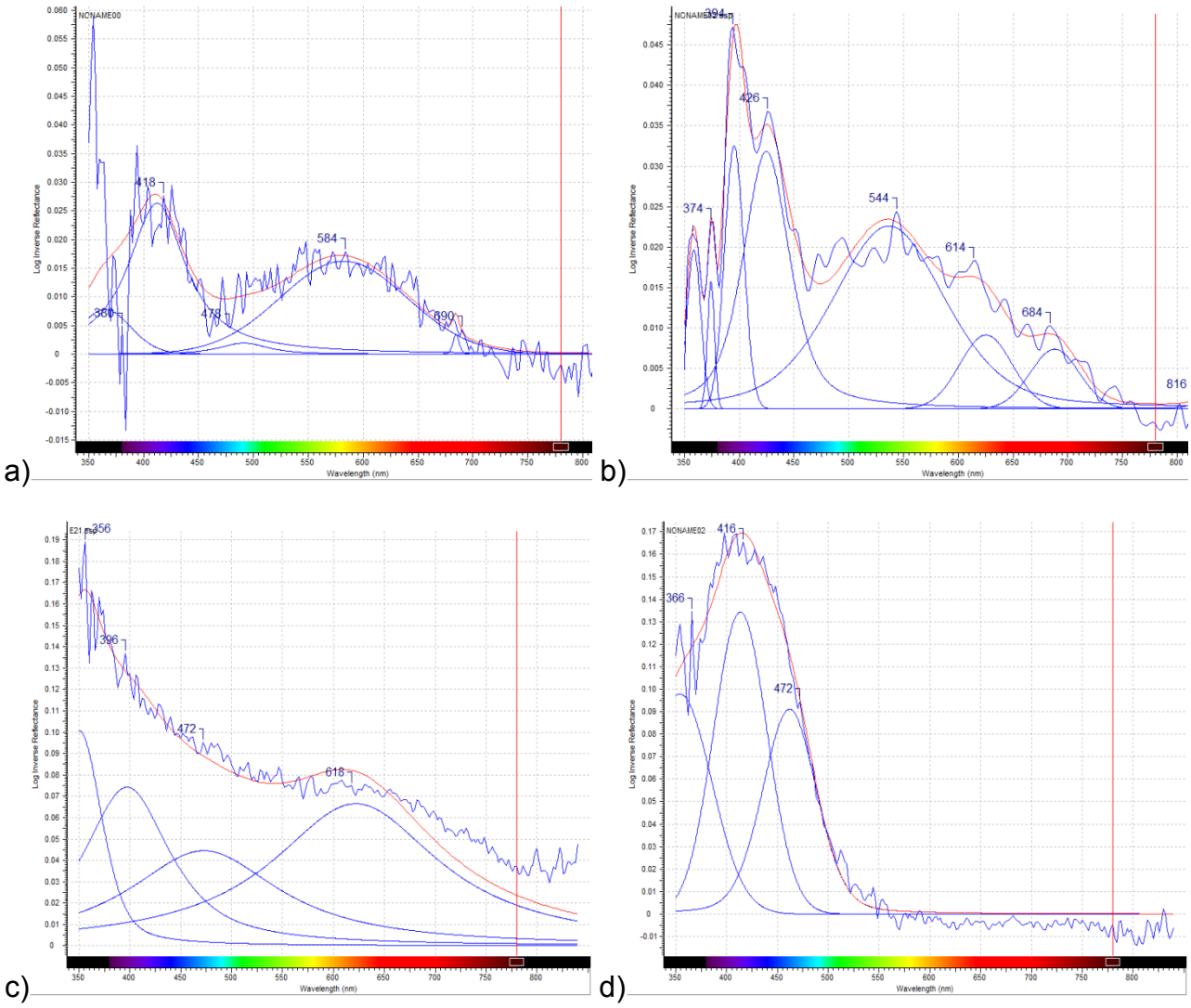

Figure 3 *UV-Visible spectra of some of the analyzed paper samples. a) Kirkland Signature (Mexico, C01), b) RetroPlus50 (Canada, C02), c) Esquisse envelope (France, E21), d) Papyrus rainbow (Europe – unspecified country, E31).*

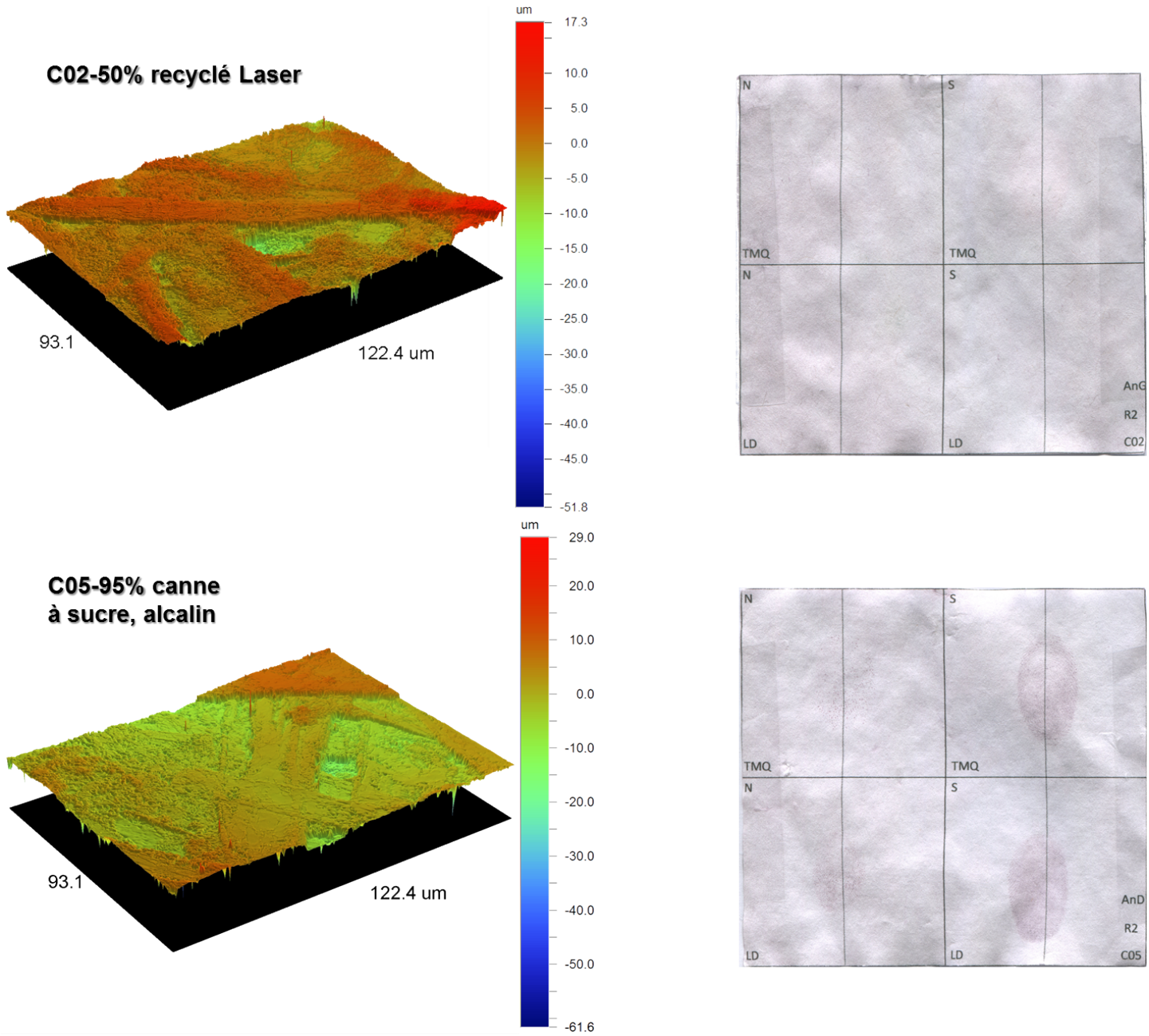

Figure 4 *Left half: 3D profiles of the RetroPlus50 (Canada; C02) and Staples Sustainable Earth Copy Paper (USA; C05) paper samples after they were processed with SMD II. Right half: illustration of the processed samples.*

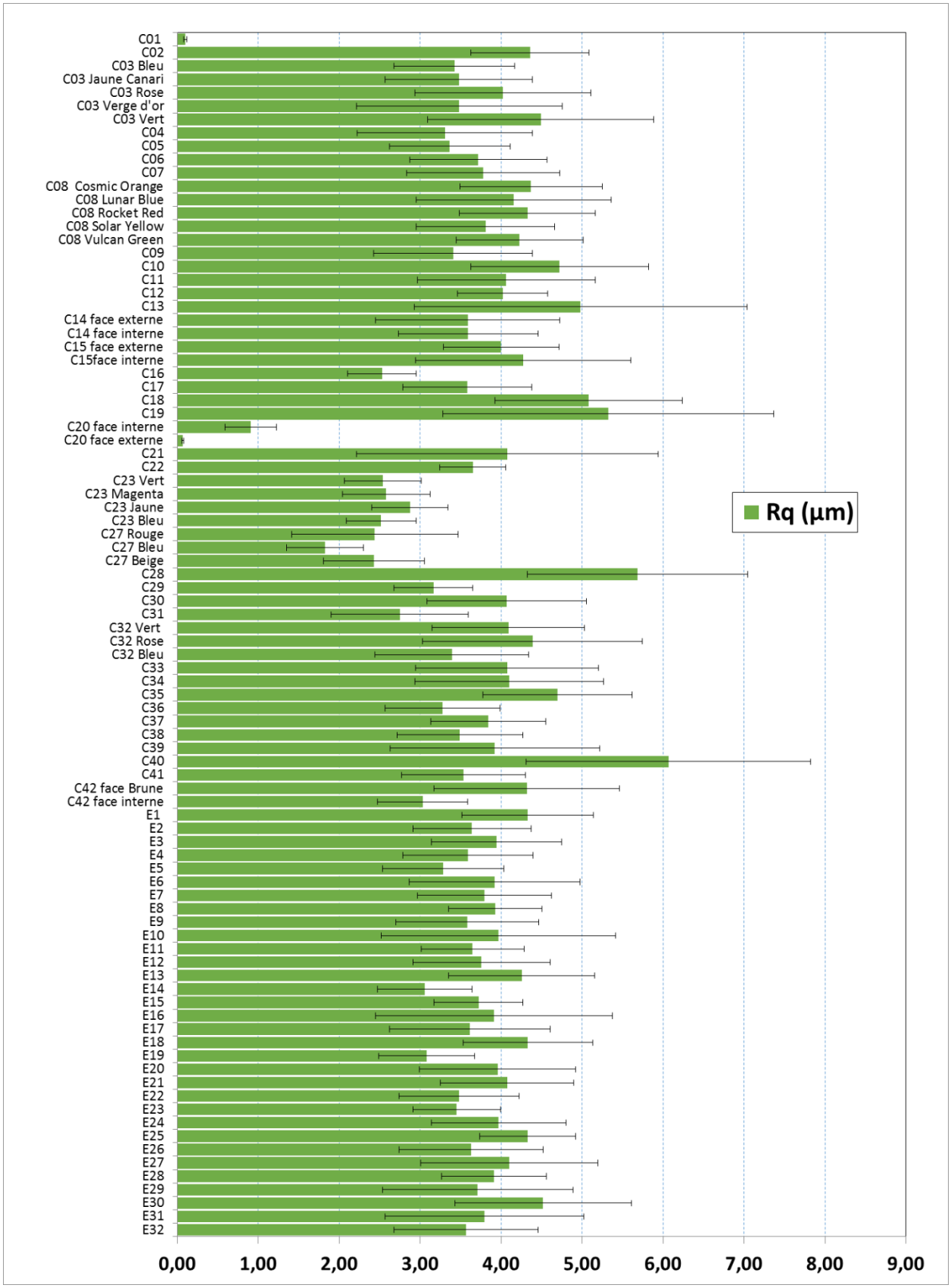

Figure 5 Average values of the Rq parameter (µm) for all the paper samples (see Appendix A for manufacturer details).

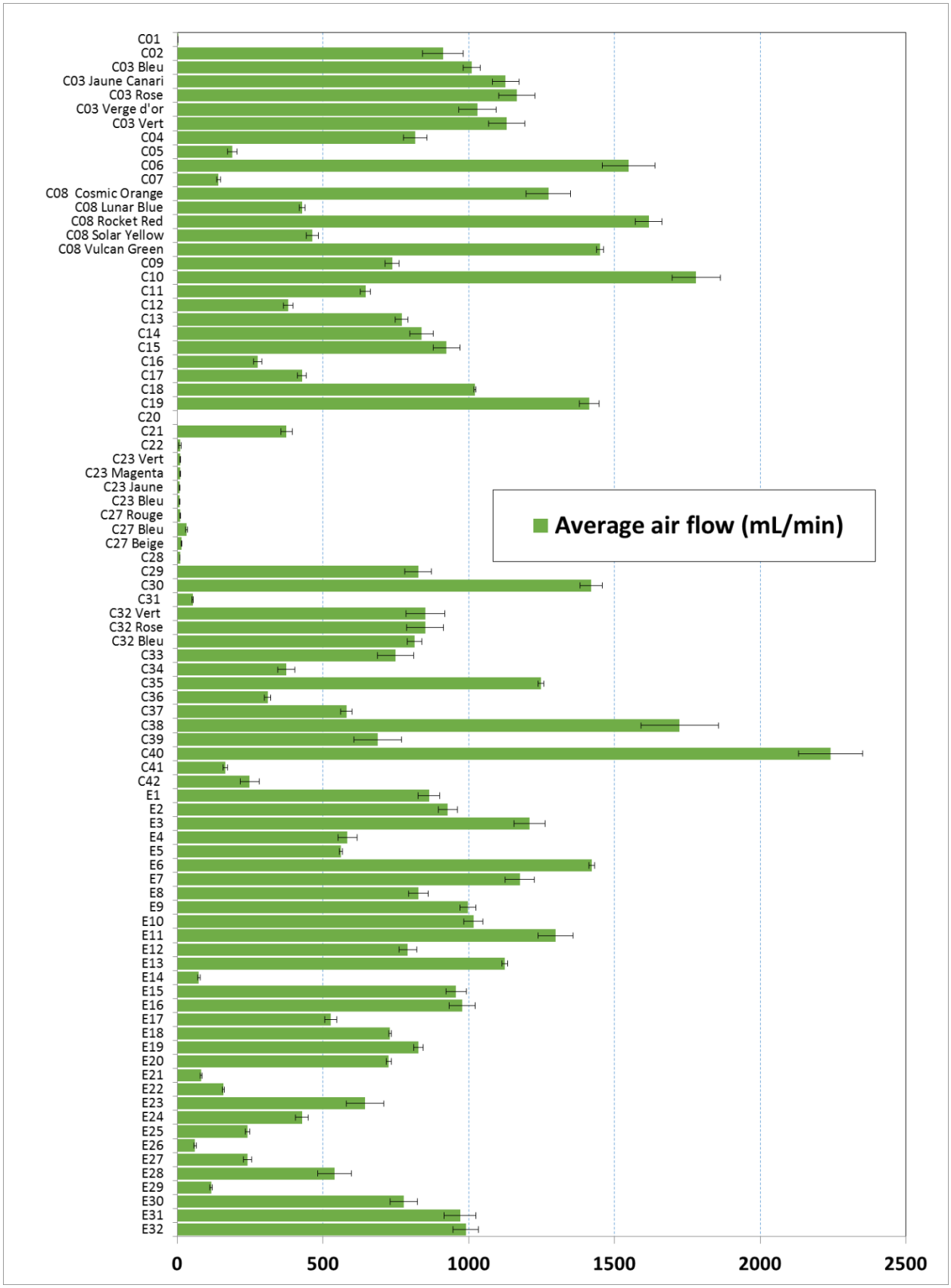

Figure 6 Average air flow (mL/min) measured for all the paper samples (see Appendix A for manufacturer details).

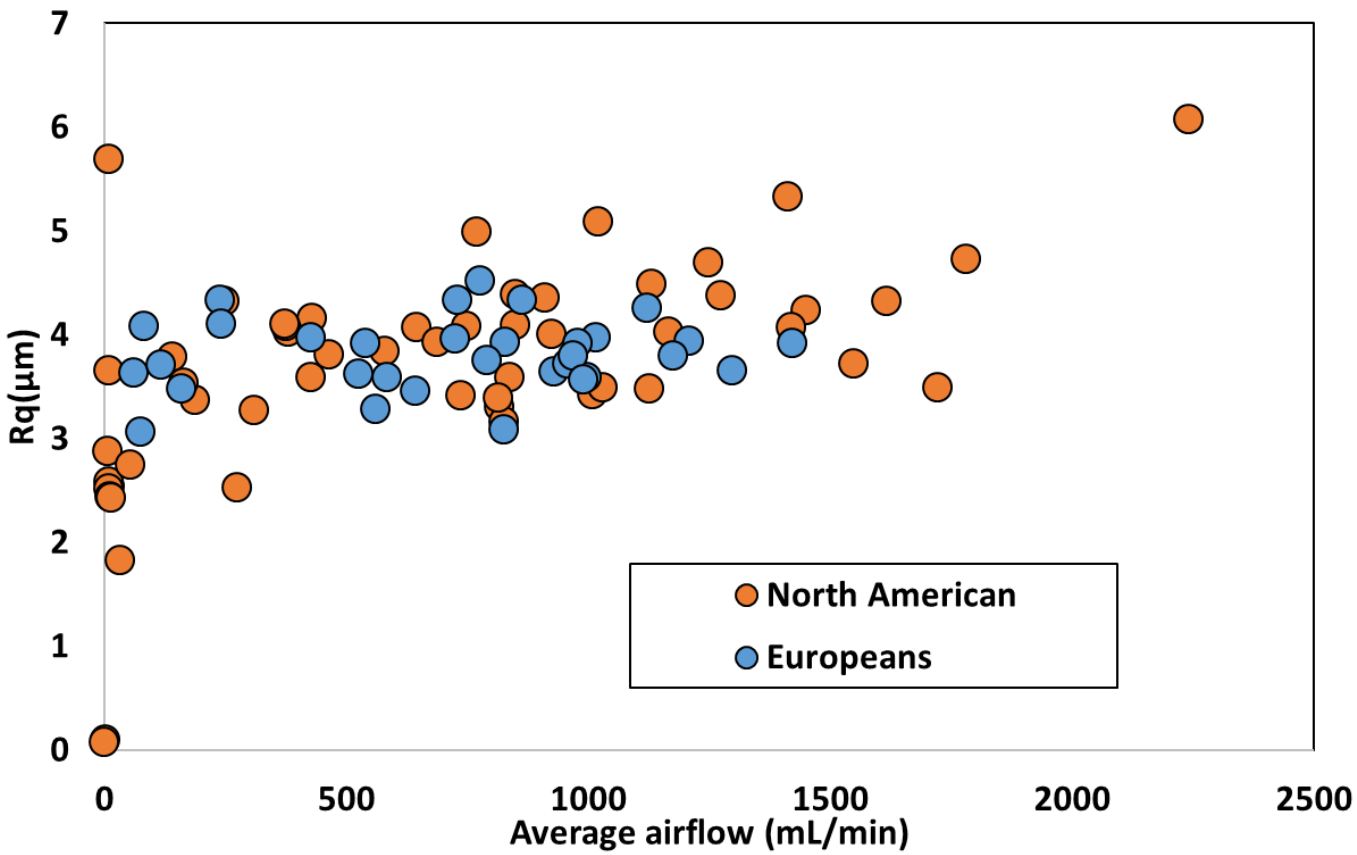

Figure 7 *Chart illustrating the relation between the average airflow (mL/min) and the Rq values (microns) for all the paper samples. Each dot represents a paper sample.*

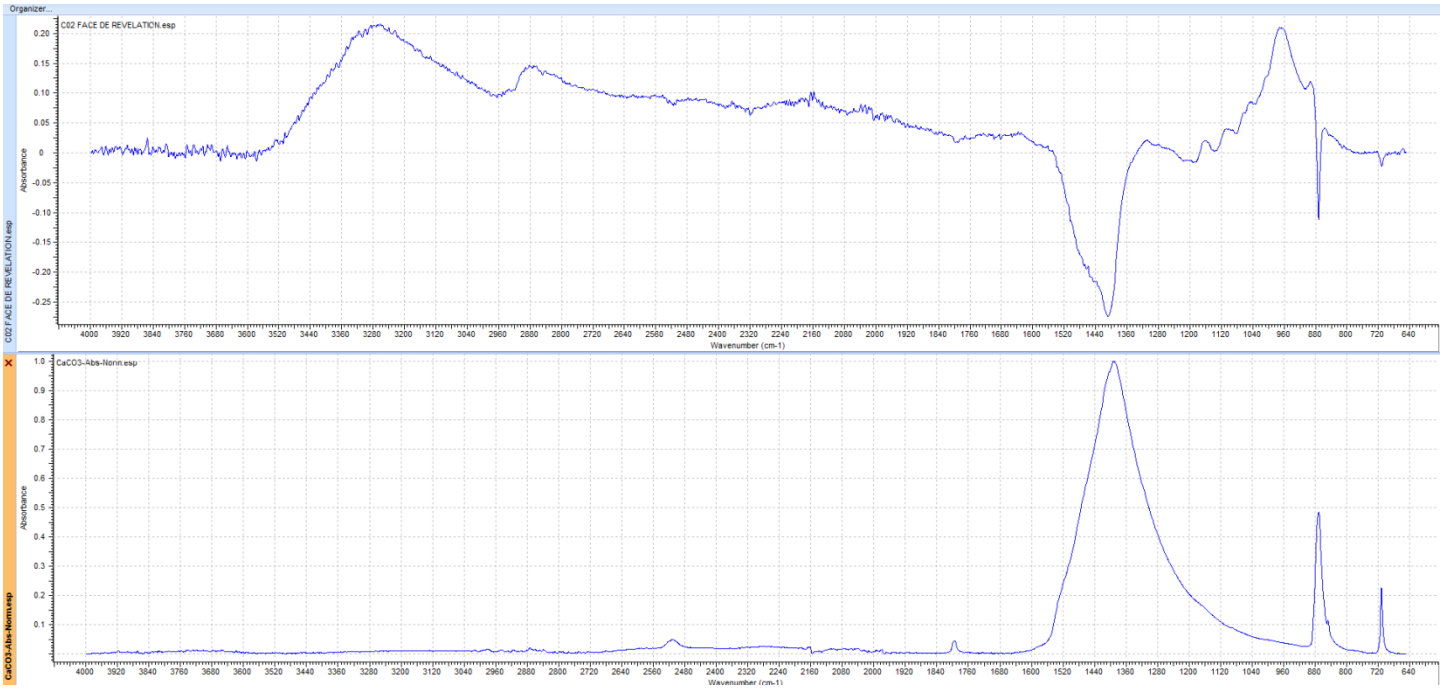

Figure 8 Top spectrum resulting from the subtraction of the IR spectra obtained before and after the application of SMD II on the paper sample RetroPlus50 Canada (C02); bottom IR spectrum corresponding to calcium carbonate.

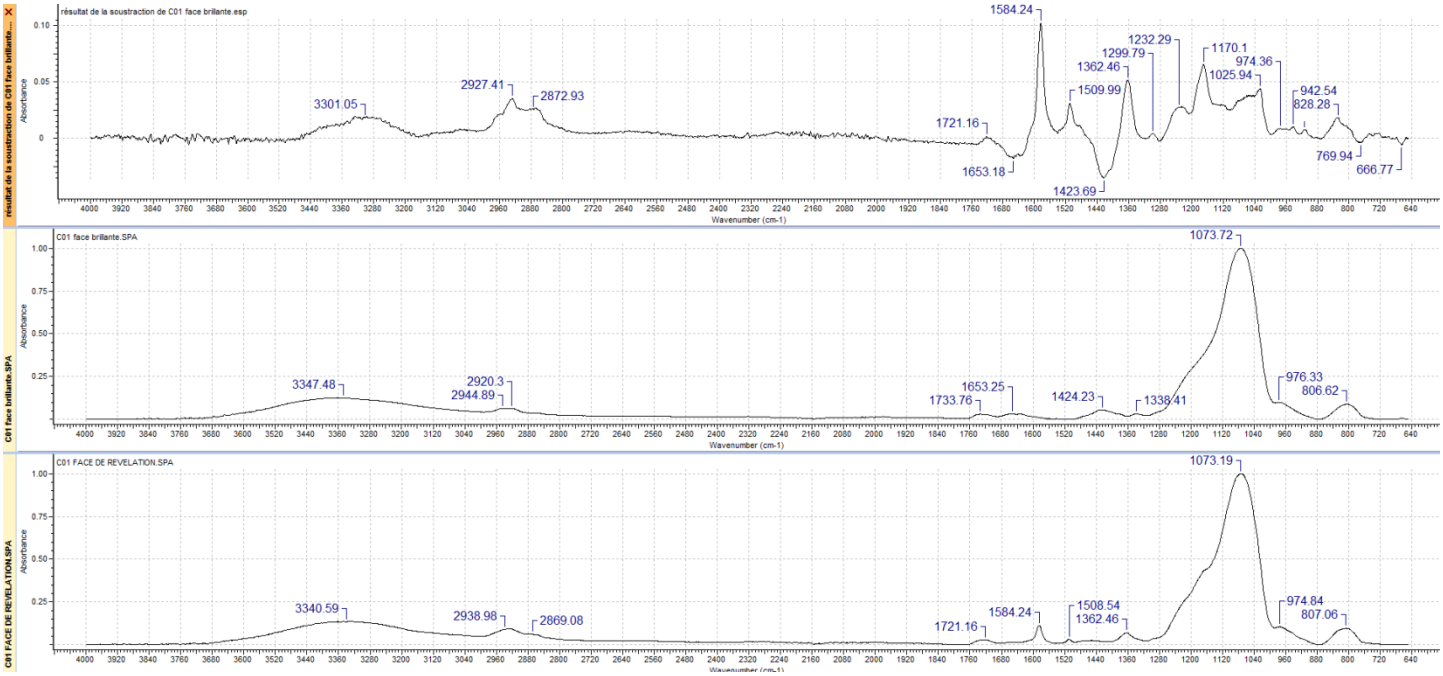

Figure 9 Top spectrum obtained by subtracting the IR spectra obtained before (middle) and after (bottom) the application of SMD II (paper sample: Kirkland Signature Mexico; C01).

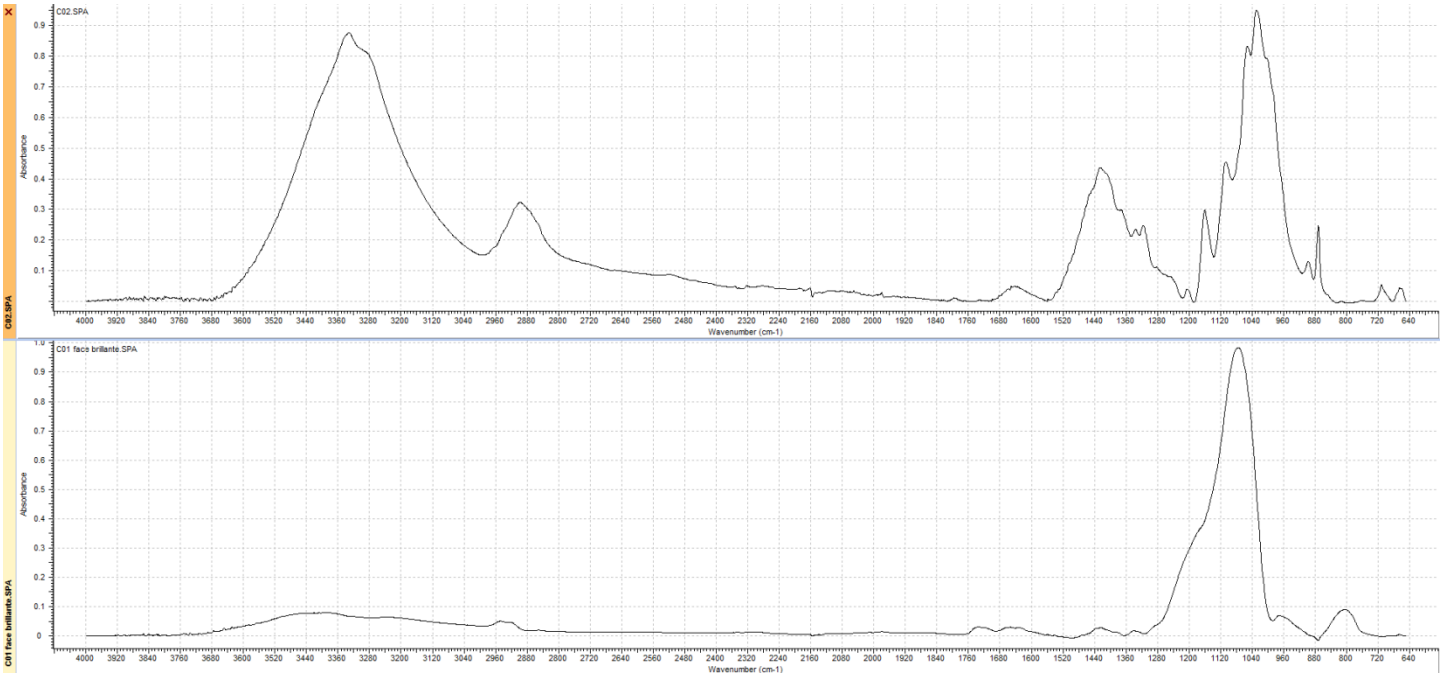

Figure 10 Difference spectra between C04 (top) and original C01 (bottom).

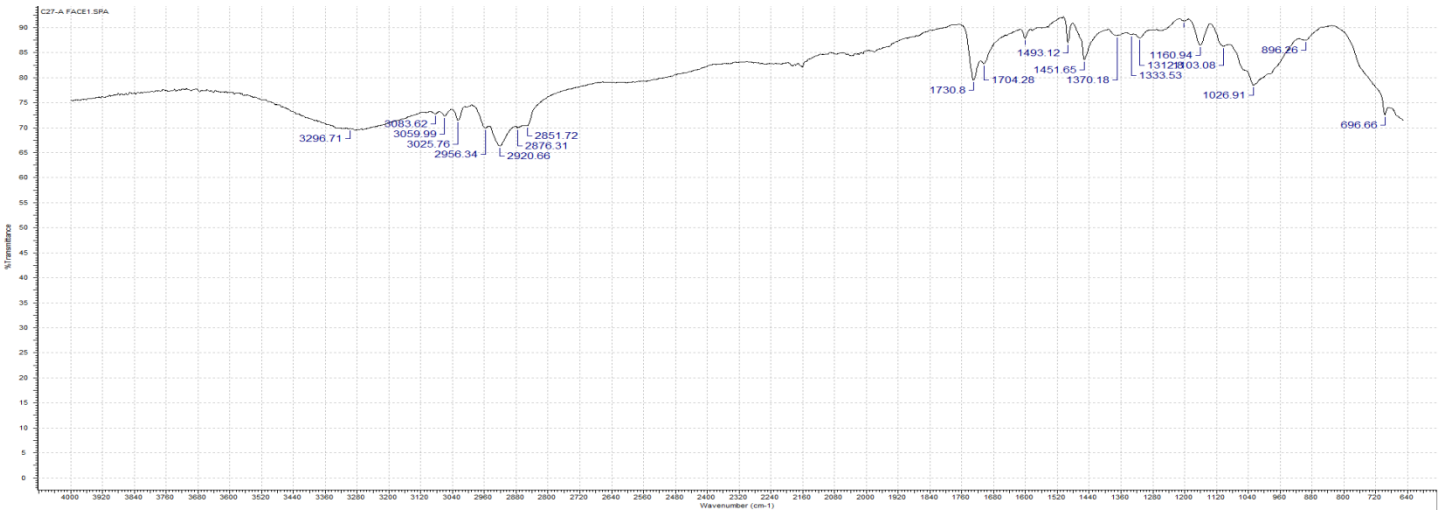

Figure 11 Infrared spectrum of the unprocessed Staples "Chemise à pochettes – 1336" paper sample (C27).

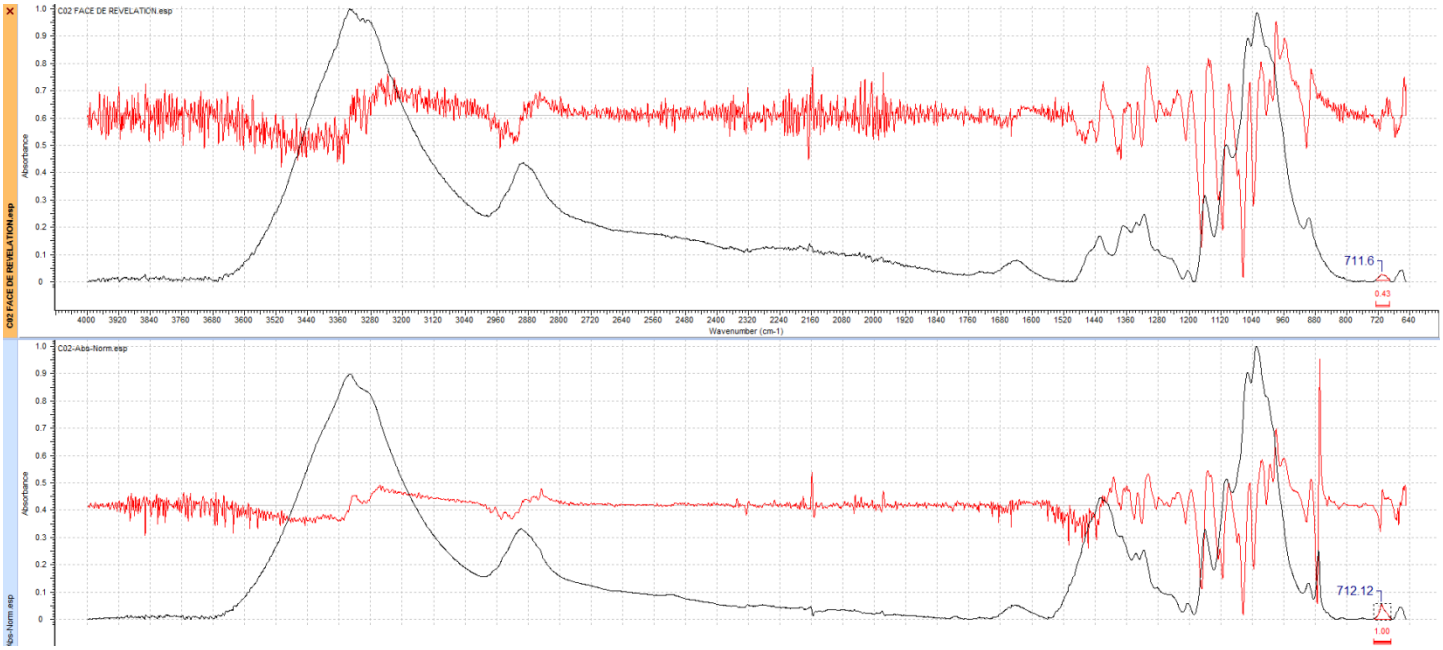

Figure 12 Derivative calculation for the RetroPlus50 paper sample (Canada; C02). Top spectra represent the paper surface with the fingermarks revealed, while bottom spectra represent the opposite surface of the same paper.

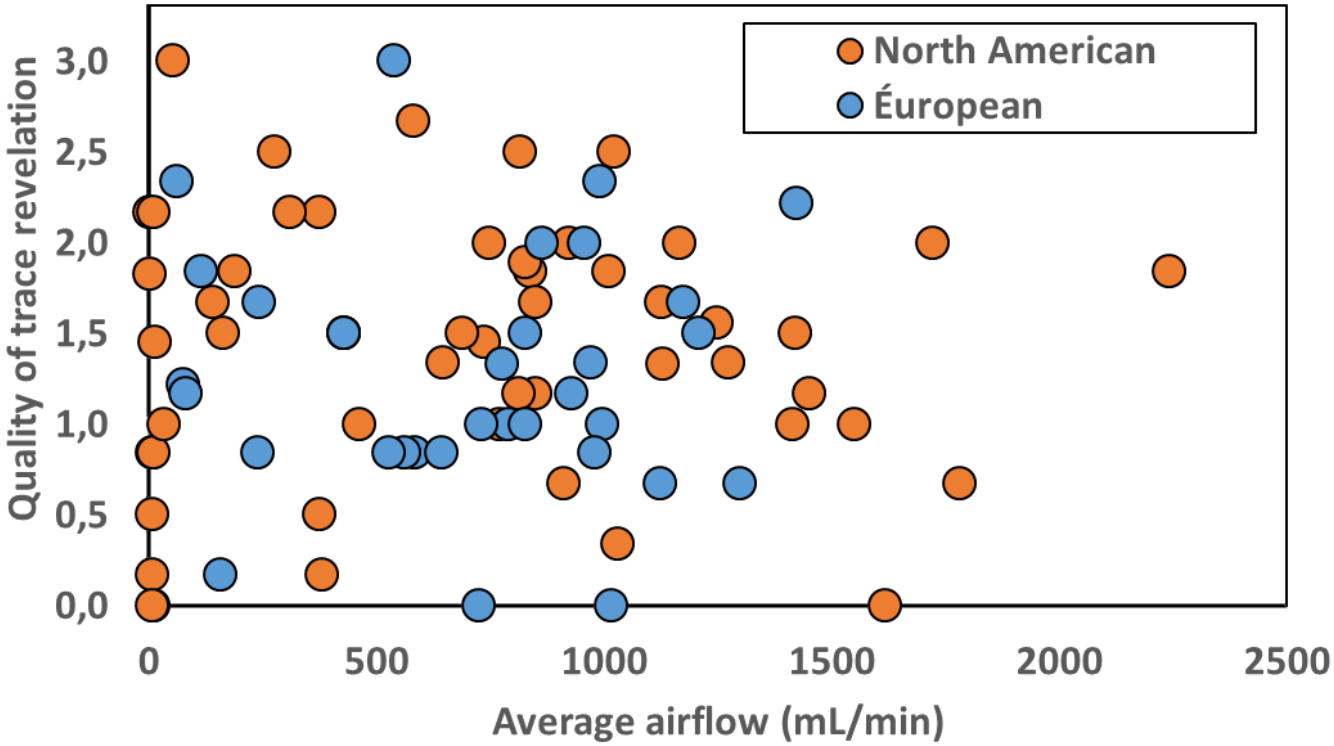

Figure 13 Chart illustrating the relation between the airflow (mL/min) and the average quality score associated with the fingermarks obtained after SMD II. Each dot represents a paper sample.

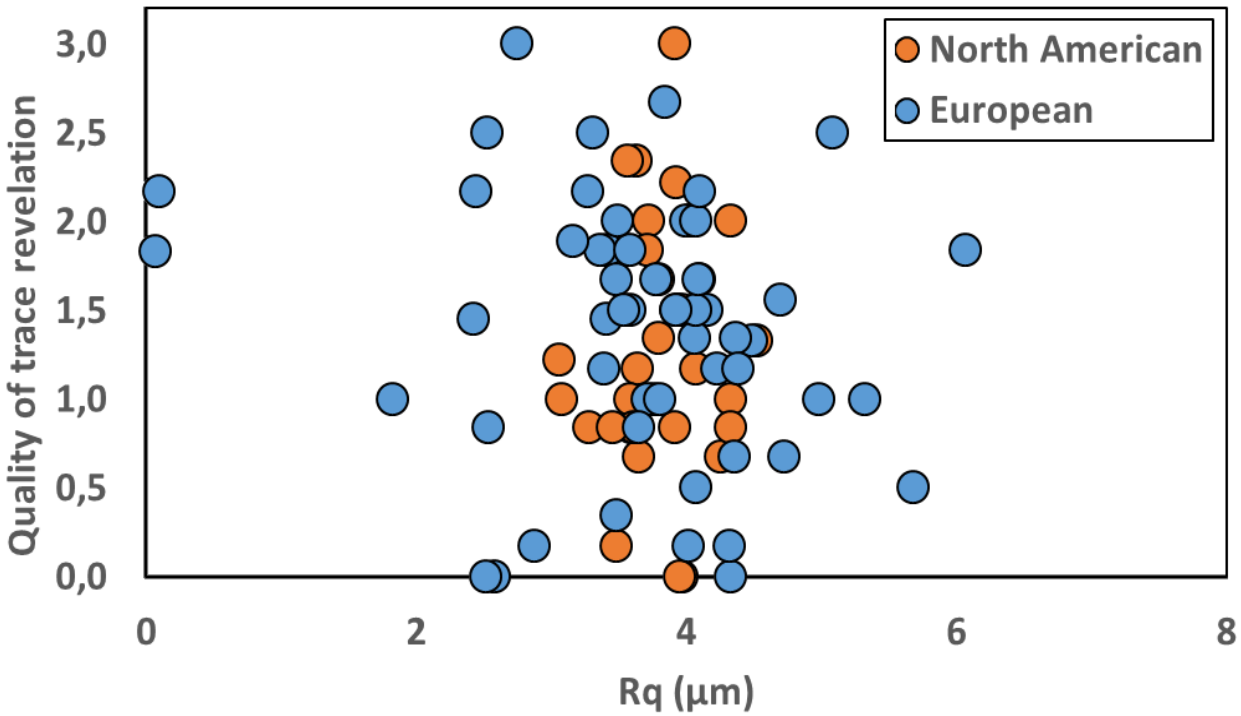

Figure 4 *Chart illustrating the relation between the Rq values (microns) and the average quality score associated with the fingermarks obtained after SMD II. Each dot represents a paper sample.*

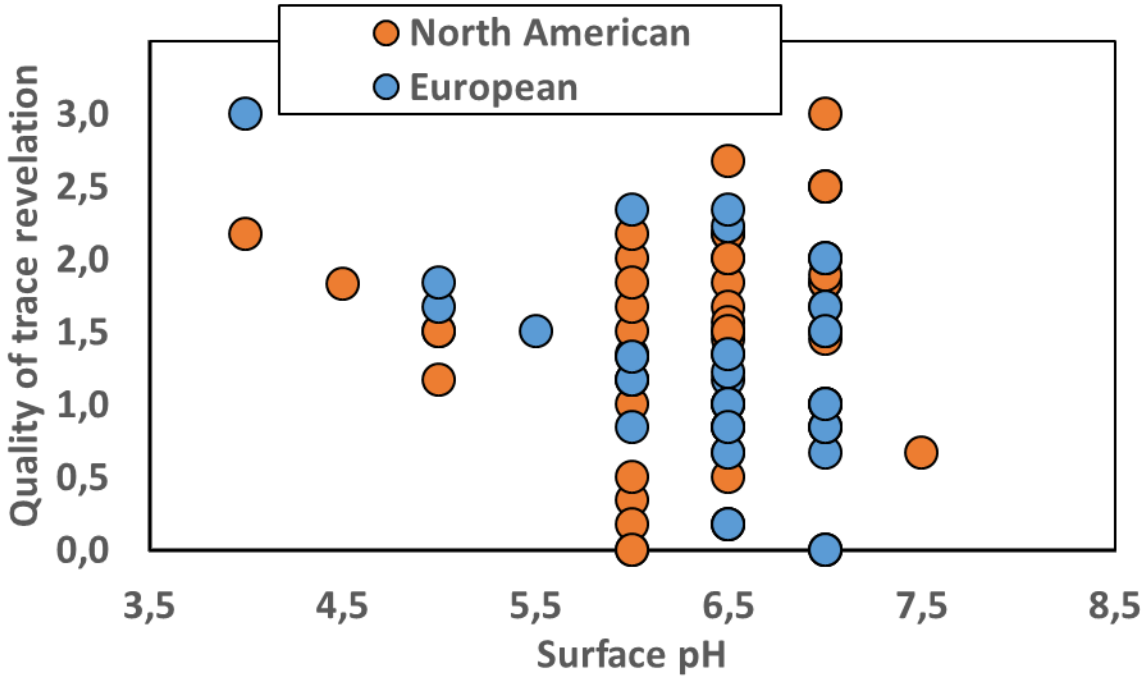

Figure 5 *Chart illustrating the relation between the surface pH and the average quality score associated with the fingermarks obtained after SMD II. Each dot represents a paper sample.*

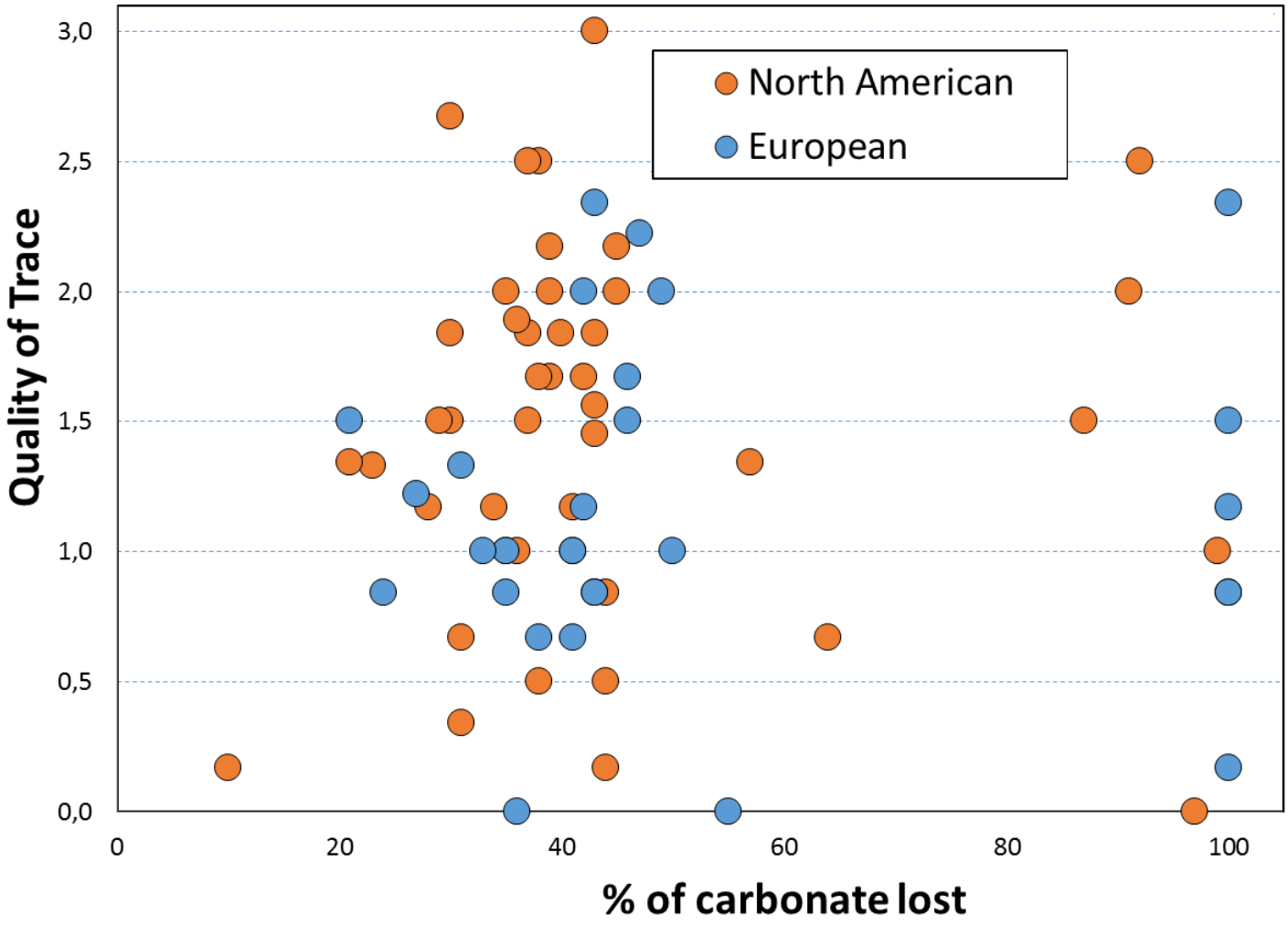

Figure 16 Chart illustrating the relation between the calcium carbonate loss (estimated %) and the average quality score associated with the fingermarks obtained after SMD II. Each dot represents a paper sample.

AUTHOR DECLARATION

We wish to confirm that there are no known conflicts of interest associated with this publication and there has been no significant financial support for this work that could have influenced its outcome.

We confirm that the manuscript has been read and approved by all named authors and that there are no other persons who satisfied the criteria for authorship but are not listed. We further confirm that the order of authors listed in the manuscript has been approved by all of us.

We confirm that we have given due consideration to the protection of intellectual property associated with this work and that there are no impediments to publication, including the timing of publication, with respect to intellectual property. In so doing we confirm that we have followed the regulations of our institutions concerning intellectual property.

We further confirm that any aspect of the work covered in this manuscript that has involved either experimental animals or human patients has been conducted with the ethical approval of all relevant bodies and that such approvals are acknowledged within the manuscript.

We understand that the Corresponding Author is the sole contact for the Editorial process (including Editorial Manager and direct communications with the office). He/she is responsible for communicating with the other authors about progress, submissions of revisions and final approval of proofs. We confirm that we have provided a current, correct email address which is accessible by the Corresponding Author and which has been configured to accept email from ForensicChemistry@elsevier.com.

Signed by authors as follows:

Name	Date	Signature
Sylvain ROBERT	July 3, 2018	
Frank CRISPINO	July 4, 2018	
Sébastien MORET	July 7, 2018	
Andy BÉBUE	July 12, 2018	

In case more space is needed, please attach a second page.

Appendix A: Paper samples

North American papers (C) and European papers (E). Laser (L), inkjet (I), Offset (O), copier/printer (P), utility (U). Recycled (R) with percentage when available, Forest Stewardship Council approved (FSC). Whiteness (%) and color also indicated. Basis weight units: $g.m^{-2}$. Some paper types, as well as basis weight, were not indicated by the suppliers.

Code	Origin	Company/Brand	Specification	Type	Use	Color	Basis weight	Surface pH
C01	Mexico	Kirkland	Signature - Professionnel Brillant	-	I	White	255	4
C02	Canada	ReproPlus50	-	R 50%	I and L	White	75	8
C03	USA	Staples	Pastel	R 30% - Acid free	P	Golden rofd, canary yellow, pink, blue, green	75	7
C04	Canada	Domtar	EarthChoice - Office paper	Mixed	P	White 92%	75	8
C05	USA	Staples	Sustainable Earth - Copy paper	95% sugar cane - Alkaline	P	White 92%	75	7
C06	USA	hp	Multipurpose paper	Mixed	P	White 96%	75	7
C07	Canada	Prairie Pulp & Paper Inc.	Step Forward Paper	80% corn / 20% FSC	P	White 92%	80	7
C08	USA	Neenah Paper Inc.	Astrobrights - Creative Expression	Acid free, lignin free	L, I, O, P	Solar Yellow, Vulcan Green, Cosmic Orange, Lunar Blue, Rocket Red	89	7
C09	USA	hp	LaserJet Paper	-	L, I, O, P	White 98%	90	7
C10	USA	Neenah Paper Inc.	Southworth - Parchemin	Mixed FSC	I and L	Ivory	90	7
C11	USA	Neenah Paper Inc.	Southworth - Granité	Mixed FSC	I and L	Ivory	90	7
C12	USA	Neenah Paper Inc.	Southworth - Lin	Mixed FSC	I and L	White	90	7
C13	USA	Neenah Paper Inc.	Southworth -Vergé antique	Mixed FSC	I and L	White	90	7
C14	Canada	Domtar	Business - Papier à lettre	R 20%	L, I, P	Venice	90	7
C15	Canada	Domtar	Business - Papier à lettre	R 20%	L, I, P	Windsor Marble	90	7

Code	Origin	Company/Brand	Specification	Type	Use	Color	Basis weight	Surface pH
C16	USA	hp	Premium Choice - Laser Paper	-	L	White 98%	120	7
C17	USA	Canon	Matte Photo Paper - MP-101	-	I	White	170	7
C18	USA	Staples	Papier à cartes	Acid and lignin free	L, I, P	Beige	250	7
C19	USA	Neenah Paper Inc.	Southworth - Parchemin (couverture)	Mixed FSC	I, L	Ivory	250	7
C20	USA	Canon	Photo paper Plus Glossy II - PP201	-	I	White	275	5
C21	USA	Staples	Tablette de papier perforé quadrillé - 22833	-	U	White	n/a	7
C22	Canada	Avery	Étiquettes CD - 5692	-	L		n/a	7
C23	Canada	Avery	Étiquettes Polyvalentes Amovibles - 6476	-	I, L	Magenta, yellow, green, blue	n/a	7
C24	USA	Staples	Protège-feuilles transparents - 10523	PVC, acid and lignin free	U	-	n/a	7
C25	Canada	Carbon Products Limited	Form-Mate	-	U	-	n/a	7
C26	Canada	Avery	Étiquettes d'adresse transparentes - 15662	-	L	-	n/a	7
C27	USA	Staples	Chemise à pochettes - 1336	Cardboard	U	-	n/a	7
C28	USA	Staples	Enveloppes d'expédition à bulles 6x9 - 17723	.	U	-	n/a	7
C29	USA	Staples	Enveloppes 5 7/8 x 9 5/8 - 594487	Mixed FSC	U	White	90	7
C30	USA	Staples	Enveloppes 5 7/8 x 9 5/9 - 194490	Mixed FSC	U	White	90	7
C31	USA	Staples	Sustainable Earth - Tablettes d'écriture	80% sugar cane residues	U	White	n/a	7
C32	Canada	3M	Post-it	R	U	Pink, green, blue	n/a	7
C33	Canada	3M	Post-it	R	U	Yellow	n/a	7
C34	USA	Staples	Étiquettes d'expédition	R Cardboard	U	Yellow	n/a	6
C35	USA	Staples	Fiches lignées - 90106	R 10% Cardboard	U	White	n/a	7
C36	USA	Staples	Tablette à réglage étroit - 66186	-	U	White	n/a	7
C37	USA	Staples	Enveloppes no1 à monnaie - 530164	FSC	U	White	105	7
C38	USA	Staples	Enveloppes no10 QuickStrip - 66396	-	U	White	75	7

Code	Origin	Company/Brand	Specification	Type	Use	Color	Basis weight	Surface pH
C39	USA	Staples	Enveloppes no10 QuickStrip - 66397	-	U	Security tint	75	7
C40	Canada	UQTR	Buvard	Bleached Kraft	U	White	n/a	6
C41	Canada	UQTR	SW,HW, Eucalyptus	-	U	White	n/a	4
C42	Canada	UQTR	Kraft couché	Kraft	P	White	n/a	7
E01	Europe	Auchan	-	-	P	White	90	7
E02	Austria	Canon Black Label zero	-	-	P	White	80	7
E03	France	Carrefour	-	-	P	White	80	7
E04	Austria	Coop	-	-	U	White	80	7
E05	Switzerland	StaplesElco swizerland Prestige	-	-	U	White	80	7
E06	France	Hp Home & Office	-	-	P	White	80	7
E07	Portugal	Inacopia Office	-	-	P	White	75	7
E08	Portugal	Inacopia Office	-	-	P	White	80	7
E09	Switzerland	Mbudget	-	-	U	White	70	7
E10	Europe	Mbudget	-	-	P	White	80	7
E11	Austria	Office	-	-	P	White	80	7
E12	Switzerland	Paetria Migos	-	-	U	White	100	7
E13	Sweden	Paetria Migos	-	-	P	White	80	7
E14	France	Paetria Premium Migos	-	-	P	White	160	7
E15	Europe	Papyrus Piano Speed	-	-	P	White	80	7
E16	Europe	Paper Team	-	-	P	White	80	7
E17	Austria	Prix Garantie Coop	-	-	U	White	70	7
E18	Germany	Sigel Office Paper Premium	-	-	P	White	80	7
E19	France	Xerox	-	-	P	White	90	7
E20	Finland	Xerox Business	-	-	P	White	80	7
E21	France	Esquisse	Envelope	R	U	Grey	80	6

Code	Origin	Company/Brand	Specification	Type	Use	Color	Basis weight	Surface pH
E22	France	La Couronne	Envelope	R	U	Brown	90	7
E23	Austria	Oecoplan coop	-	R	U	Beige	80	6
E24	France	Papeteria	-	R	P	Grey	80	6
E25	Germany	Paper Union Inapa	-	R	P	Grey	80	7
E26	Switzerland	Raygan Aligro	-	R	P	Beige	n/a	6
E27	France	Paetria	-	-	P	Pink	80	7
E28	France	Paetria	-	-	P	Yellow	80	7
E29	France	Paetria	-	-	P	Green	80	7
E30	Europe	Papyrus Rainbow	-	-	P	Pink	80	7
E31	Europe	Papyrus Rainbow	-	-	P	Yellow	80	7
E32	Europe	Papyrus Rainbow	-	-	P	Green	80	7

Appendix B: Samples of fingermarks revelations using SMDII

Four fingerprint traces were placed on each paper sample. In the upper part are traces of the first donor, in the lower part, the traces of the second donor. In the left part, the traces are natural. In the right part, the traces are loaded (passage of the fingers on the forehead and the neck to increase the quantity of secretion of the trace). Original samples are on the right, and post-revelation samples are on the left.

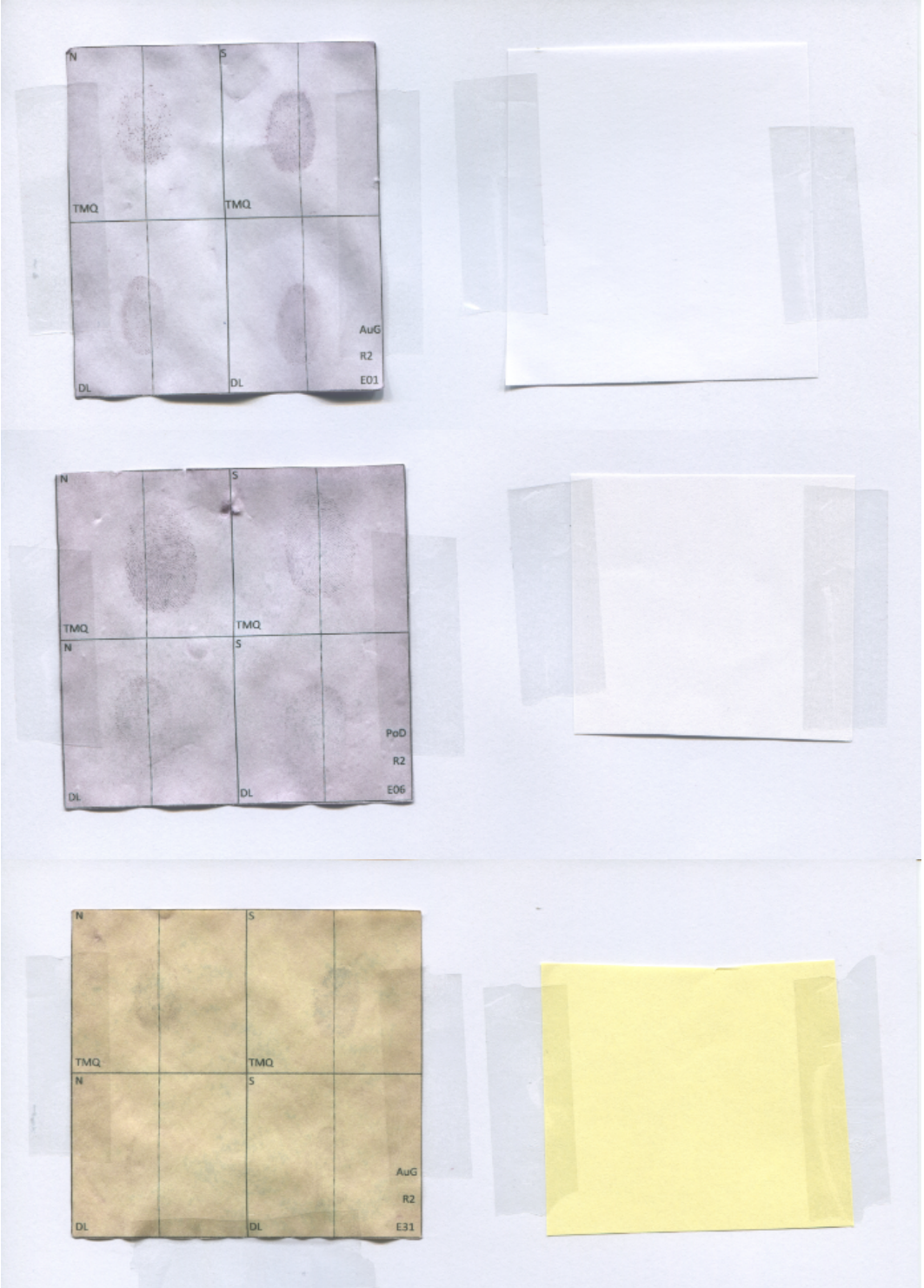

Appendix C: Rq pre and post-revelation of papers

Samples	Rq pre-revelation	Rq post-revelation	Difference
C01	0.097	0.968	0.870
C02	4.357	4.772	0.415
C03 Bleu	3.422	4.627	1.205
C03 Jaune Canari	3.479	5.647	2.168
C03 Rose	4.022	4.861	0.839
C03 Verge d'or	3.483	4.552	1.069
C03 Vert	4.489	5.654	1.165
C04	3.307	3.842	0.535
C05	3.366	4.901	1.535
C06	3.717	5.347	1.630
C07	3.779	4.791	1.012
C08 Cosmic Orange	4.370	5.015	0.645
C08 Lunar Blue	4.156	3.633	0.523
C08 Rocket Red	4.325	4.824	0.499
C08 Solar Yellow	3.808	4.341	0.533
C08 Vulcan Green	4.228	5.192	0.964
C09	3.407	4.186	0.779
C10	4.723	4.186	0.537
C11	4.063	5.934	1.871
C12	4.020	4.730	0.710
C13	4.983	5.884	0.901
C14	3.588	4.004	0.416
C15	4.000	4.149	0.149
C16	2.530	3.812	1.282
C17	3.582	5.879	2.297
C18	5.082	5.144	0.062
C19	5.323	6.498	1.175
C20	0.068	0.402	0.334
C21	4.076	3.507	0.569
C22	3.651	3.472	0.179
C23 Bleu	2.517	3.827	1.310
C23 Jaune	2.876	3.177	0.301
C23 Magenta	2.582	3.637	1.055
C23 Vert	2.538	2.974	0.436
C27 Beige	2.429	3.074	0.645
C27 Bleu	1.825	2.825	1.000
C27 Rouge	2.440	2.759	0.319
C28	5.685	6.245	0.560
C29	3.163	4.728	1.565
C30	4.069	6.450	2.381
C31	2.748	3.110	0.362
C32 Bleu	3.391	4.769	1.378

Samples	Rq pre-revelation	Rq post-revelation	Difference
C32 Rose	4.387	4.483	0.096
C32 Vert	4.089	4.086	0.003
C33	4.074	3.933	0.141
C34	4.098	4.694	0.596
C35	4.696	4.875	0.179
C36	3.274	3.556	0.282
C37	3.842	3.395	0.447
C38	3.492	4.269	0.777
C39	3.923	5.342	1.419
C40	6.069	6.105	0.036
C41	3.534	3.877	0.343
C42	4.317	4.971	0.654
E1	4.331	3.688	0.643
E10	3.970	4.069	0.099
E11	3.649	4.414	0.765
E12	3.756	3.845	0.089
E13	4.254	3.998	0.256
E14	3.059	4.447	1.388
E15	3.720	4.955	1.235
E16	3.911	4.332	0.421
E17	3.615	4.078	0.463
E18	4.329	4.173	0.156
E19	3.080	3.577	0.497
E2	3.641	4.003	0.362
E20	3.956	3.488	0.468
E21	4.075	4.311	0.236
E22	3.480	4.046	0.566
E23	3.451	4.959	1.508
E24	3.968	4.427	0.459
E25	4.328	3.281	1.047
E26	3.633	4.056	0.423
E27	4.099	4.036	0.063
E28	3.911	3.350	0.561
E29	3.711	4.351	0.640
E3	3.941	4.573	0.632
E30	4.519	4.160	0.359
E31	3.792	4.160	0.368
E32	3.570	3.825	0.255
E4	3.589	3.932	0.343
E5	3.284	3.274	0.010
E6	3.920	3.899	0.021
E7	3.795	3.900	0.105
E8	3.927	3.883	0.044
E9	3.584	4.536	0.952